20 Years of Spectroscopy with EBIT" (Berkeley 2006)

"Anticipated X-ray and VUV Spectroscopic Data from ITER with appropriate Diagnostic Instrumentation"

R. Barnsley 1,2, I. H. Coffey 1,2, M. G. O'Mullane 1,3, H. P. Summers 1,3, N. J. Peacock 1,2.

(1) *EURATOM/UKAEA Fusion Association, Culham Science Centre, Abingdon, Oxfordshire OX14 3DB UK*.
(2) *Department of Physics and Astronomy, Queen's University of Belfast, BT7 1NN UK.*
(3) *Department of Physics and Applied Physics, University of Strathclyde, Glasgow,G4 0NG UK.*

With acknowledgements to R. Neu (IPPGarching); W. Beil (KFA Julich) and T. Pütterich (Ph D thesis 2005, Augsburg).

- **The radiation characteristics of sample elements**, H through W, in ITER have been modelled throughout the X-ray and VUV regions (0.1 -100 keV), using the diffusive ion equilibrium model SANCO and the ADAS level population code and data base.

* **Line/continuum**. Bound–bound transitions required for line profile analyses of non-fuel core ions dominate the continuum spectrum in the 0.1-10 keV region at acceptably low elemental concentrations(n_{imp}/n_e ~ few x 10^{-5} for ΔP_{rad} =500kW. The continuum is the main source of noise in the line profile analyses.

* **The spectral signature varies greatly** depending on the impurity mix and whether the viewing line-of-sight **(LOS)** encompasses the divertor and/or core regions, the assumed ion transport and the plasma operating parameters.

* **Diagnostics proposed, based on broad band** (0.1 -100 keV), low resolution $\Delta E/E$ ~ 1/20, reconstruction of the spectral signature with arbitrary impurity mix and at all r/a.

* **Divertor emission** in the XUV-VUV region.

* **Diagnostic instrumentation**. Imaging Bragg reflectors and diffractors and position-sensitive energy-resolving detectors, cover the full spatial extent of the core plasma. Estimates of the core signal/noise are based on experience with tritium experiments on JET. The divertor diagnostics make use of a suite of aspheric diffraction grating spectrometers designed to measure impurity ion influxes and are essential for plasma control.

* Oxford experiments and **Role of EBIT.**

Collection of relevant spectral lines

Elements which may be abundant in the ITER plasma:

First wall materials:	Be, C, Cu, W
Fuel:	H, D, T
Fusion product:	He
Structural materials:	Cr, Fe, Ni, …
Seeded impurities:	N, Ne, Ar, Kr
Others:	Li, O, Al, Si, Zr, Mo, …

Wavelengths of the main transitions of H- and He-like Argon, Iron and Krypton.

Ground state	Excited state	λ Ar (nm)	λ Fe (nm)	λ Kr (nm)
He-like $1s^2$	1s-2p $^1S - ^1P^0$	0.39488	0.18503	0.0946
	1s-2p $^1S - ^3P^0$	0.39691	0.18553	0.0952
	1s-2s $^1S - ^3S$	0.3994	0.18680	0.0955
	1s-3p $^1S - ^1P^0$	0.3370	0.17913	0.0805
H-like 1s	2p $^2S - ^2P^0$ J=1/2	0.3737	0.1784	0.0923
	2p $^2S - ^2P^0$ J=3/2	0.3731	0.1778	0.0918
	3p $^2S - ^2P^0$	0.3150	0.1502	0.0777

Ne- and Na-like Tungsten lines suitable for the ITER core.

Ground state	Excited state	Wavelength (nm)
W^{64+} Ne-like $2p^6\ ^1S_0$	$2p^5\ 3s^1\ ^1P_1$	0.1498
	$2p^5\ 3s^1\ ^3P_1$	0.1279
	$2p^5\ 3d^1\ ^3P_1$	0.1383
	$2p^5\ 3d^1\ ^1D_1$	0.1191
	$2p^5\ 3d^1\ ^3D_1$	0.1364
W^{63+} Na-like $3s^1\ ^2S_{1/2}$	$4p^1\ ^2P_{1/2}$	0.374
	$4p^1\ ^2P_{3/2}$	0.357

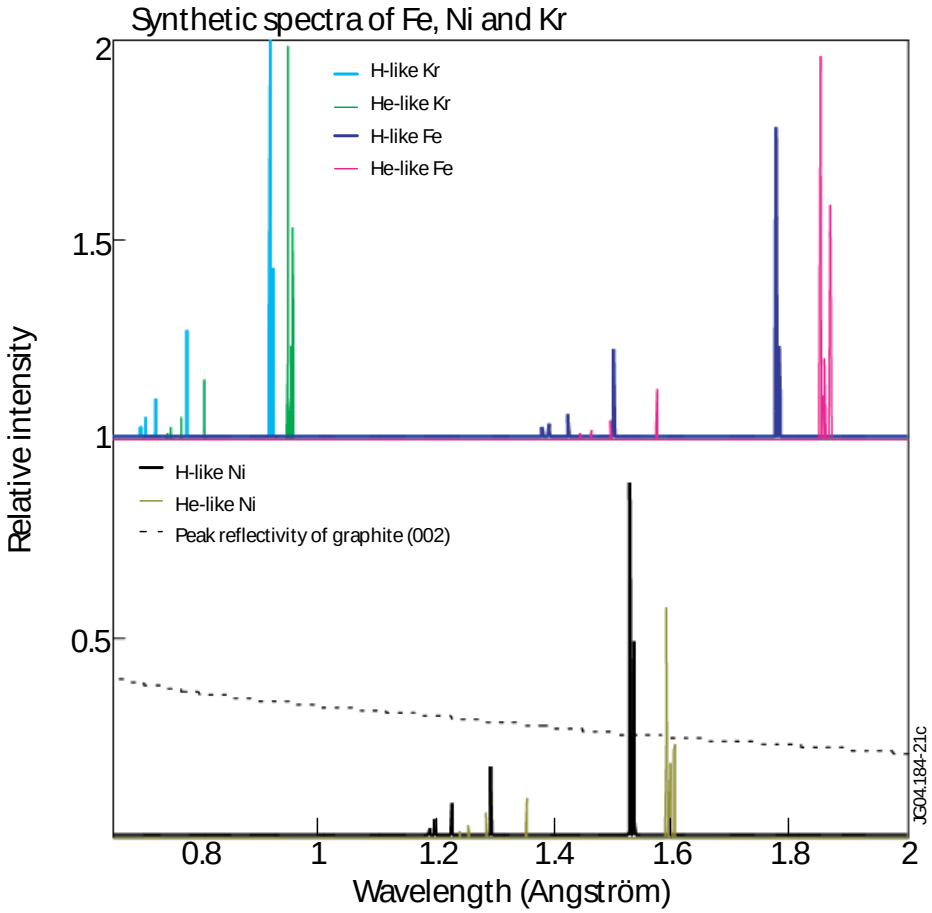

Synthetic Spectra of H- and He-like Kr, Fe, and Ni.

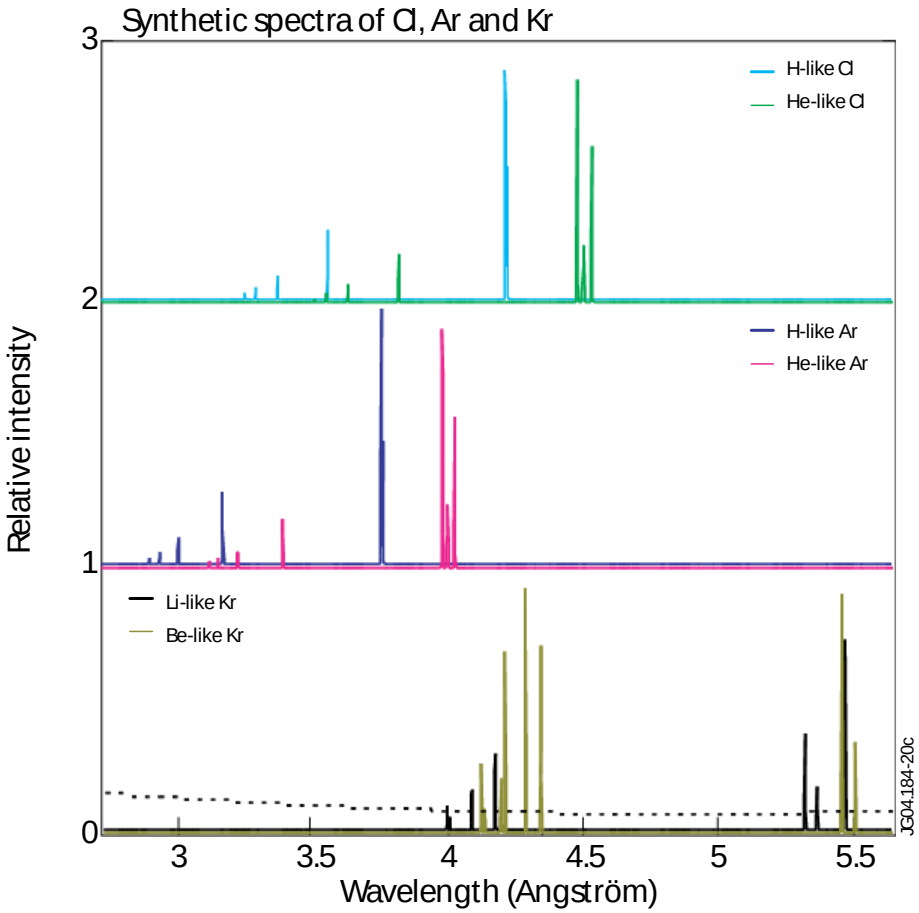

Synthetic Spectra of H- and He-like Cl and Ar and (below) Li-and Be-like Kr.

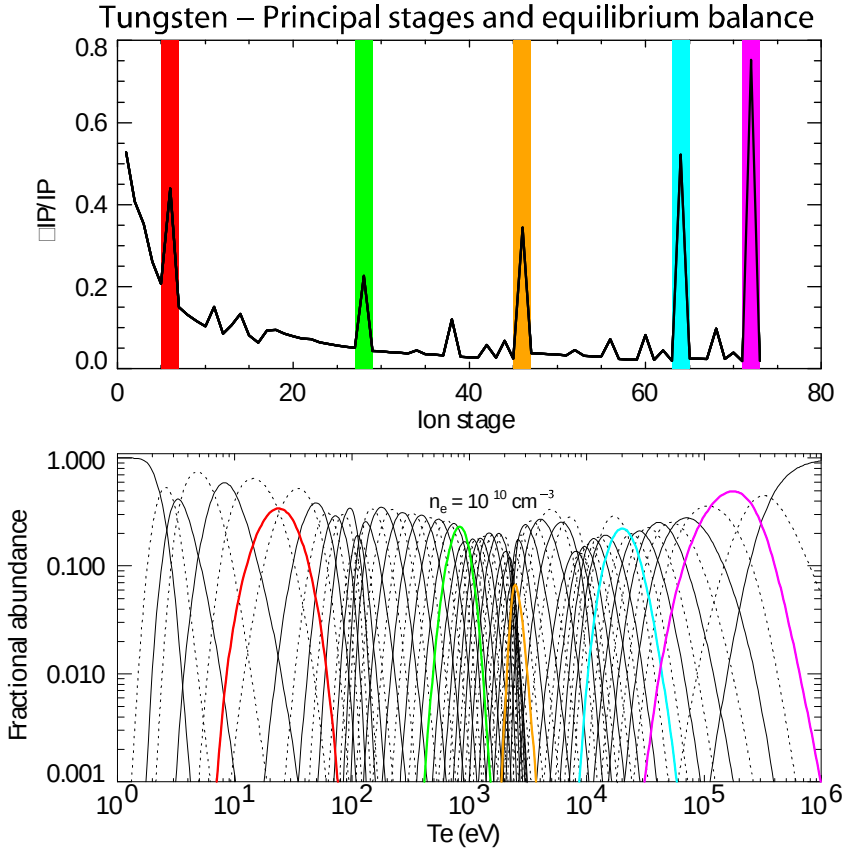

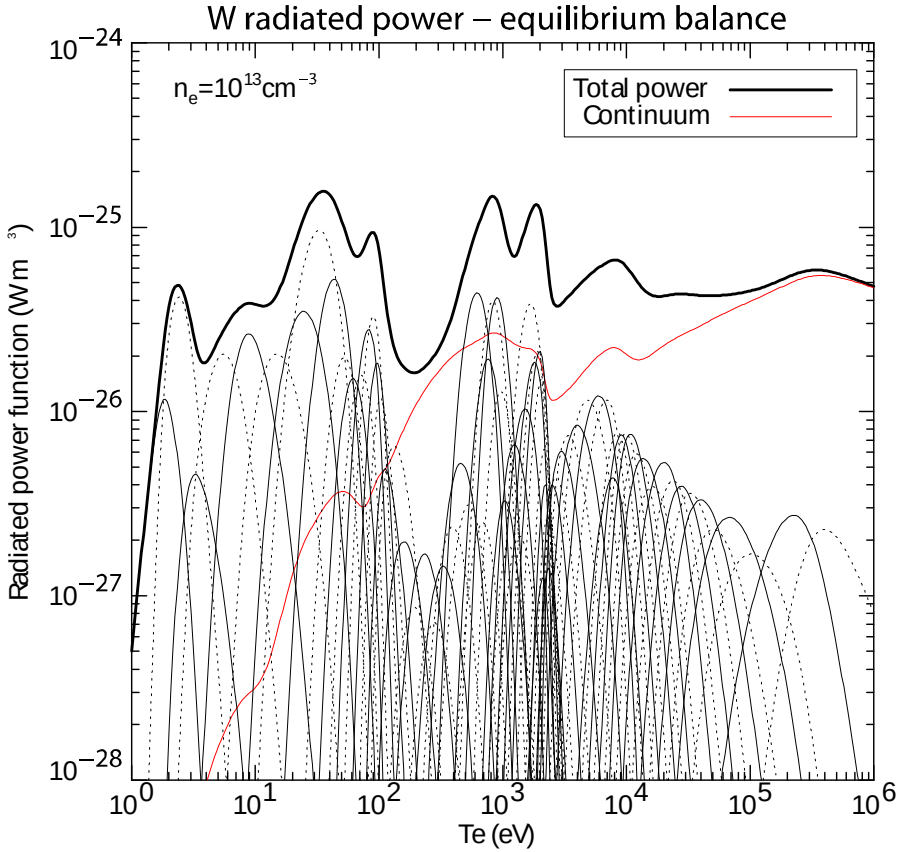

Fractional Abundances of Tungsten ions with dominant stages highlighted. RHS indicates the power contribution per Tungsten ion split into ionisation stages.

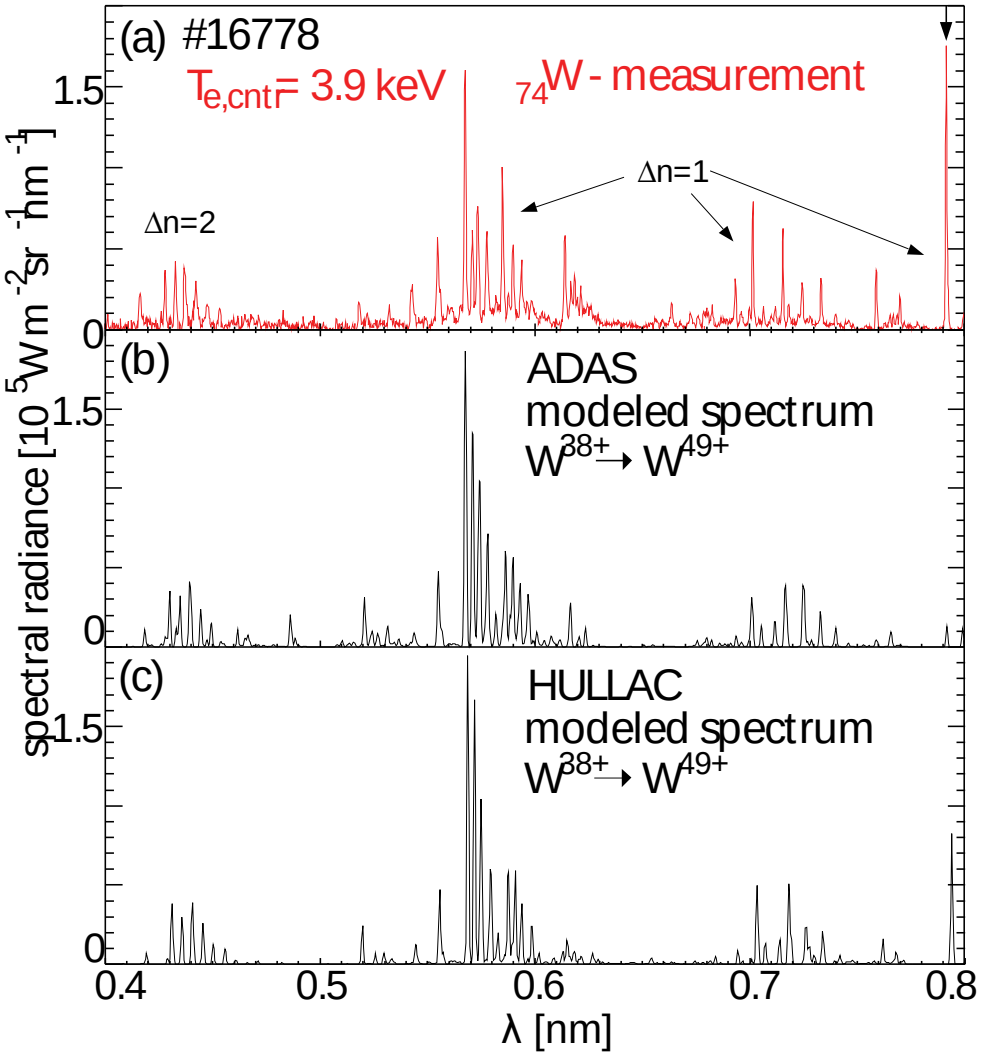

Tungsten spectrum from Asdex discharge #16778 with $N(W)/n_e \cong 2\ 10^{-4}$. E2 transition at 0.793nm due to inner-shell ionisation of Cu-like W^{45+} not modelled by ADAS. (Pütterich, 2005)

X-ray resonance lines in ITER relative to background continua.

Lighter elements e.g. Ar, Fe offer better signal above background than Kr.

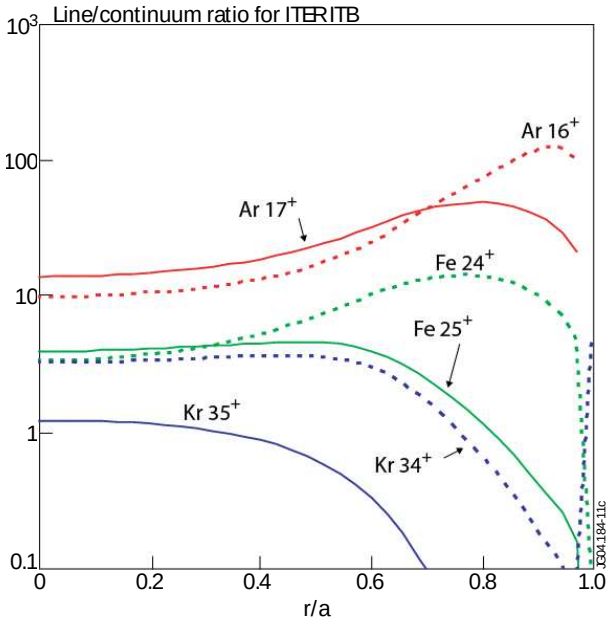

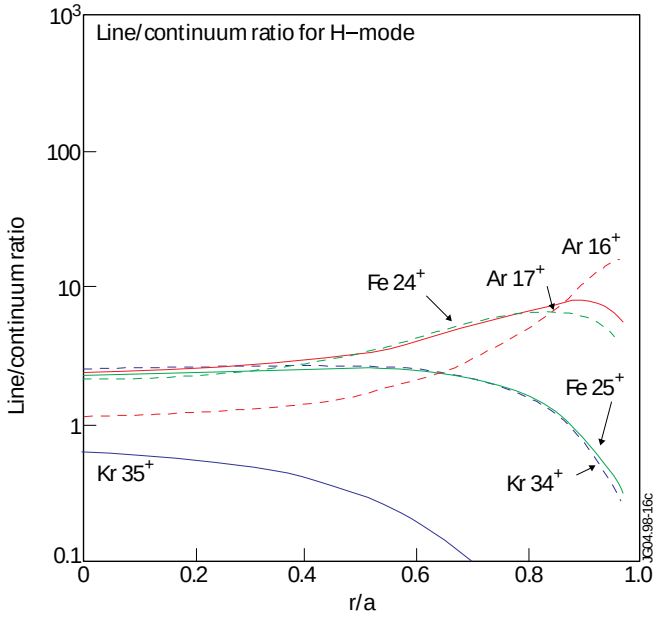

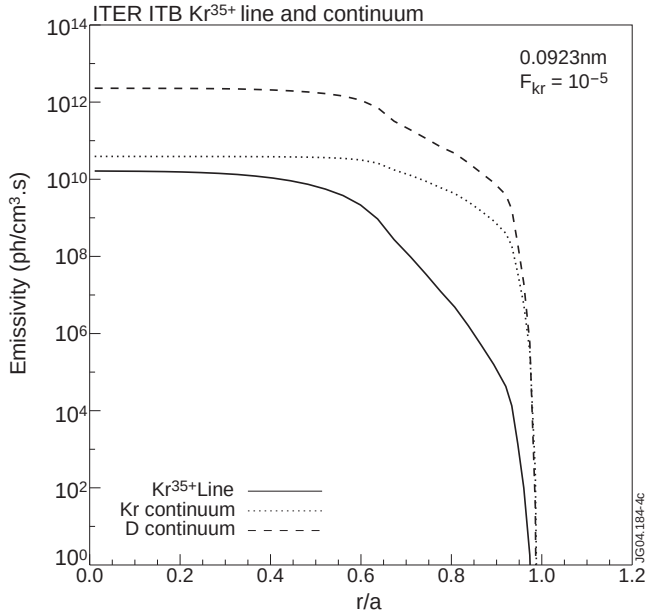

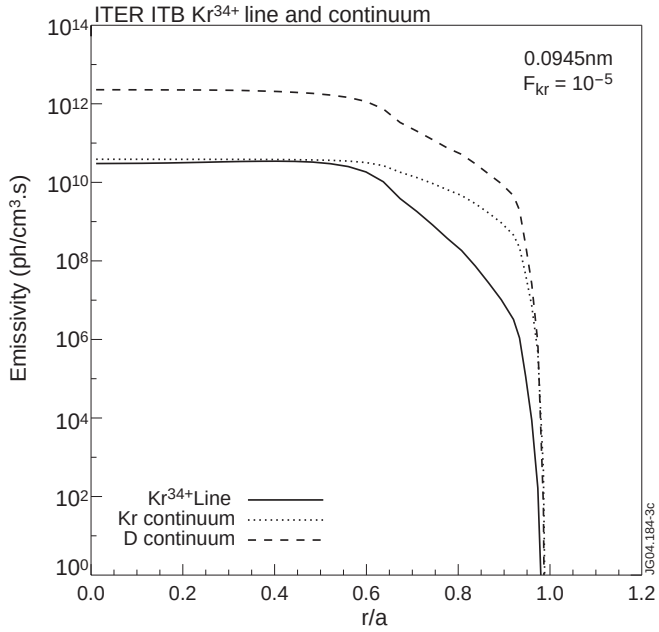

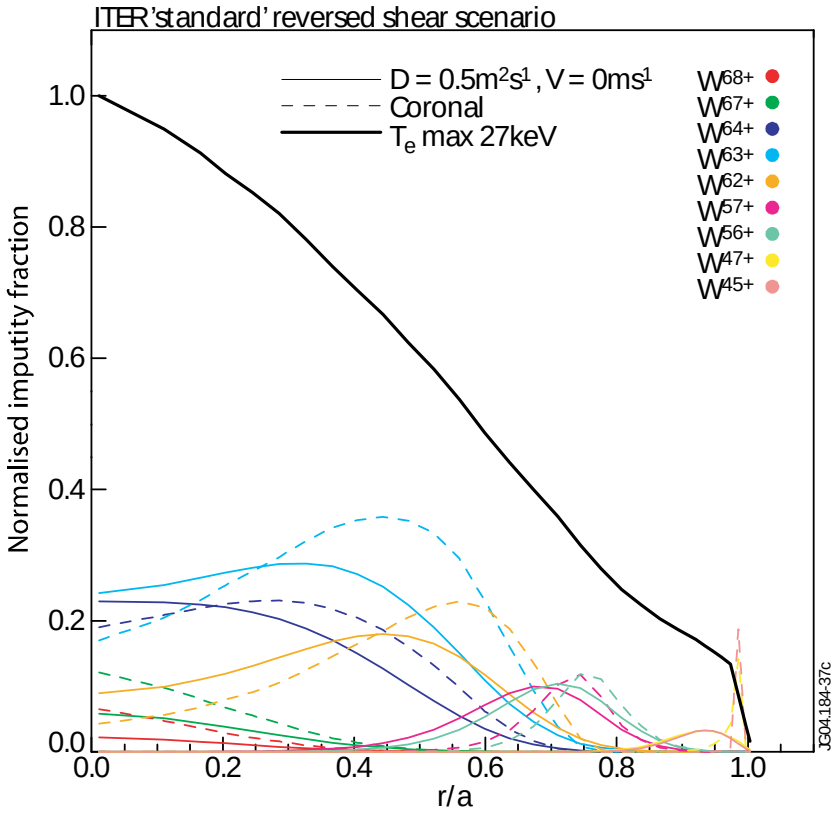

Fractional abundance of W ions.

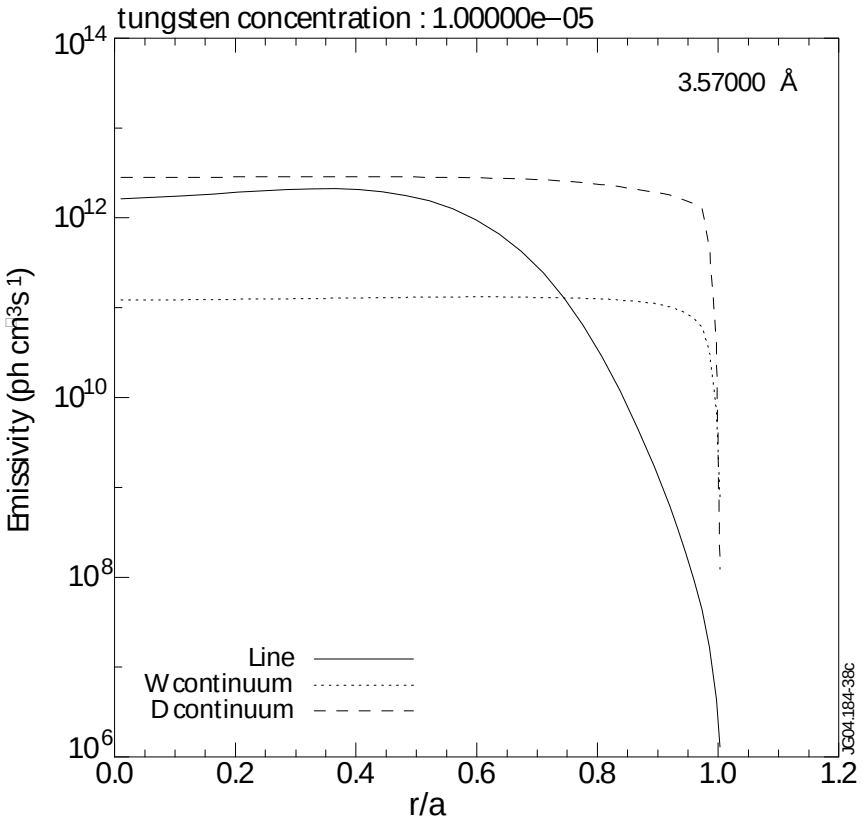

W^{63+} Volume emissivity

SANCO-modelled ITB plasma with tungsten for $n_w = 10^{-5}.n_e$

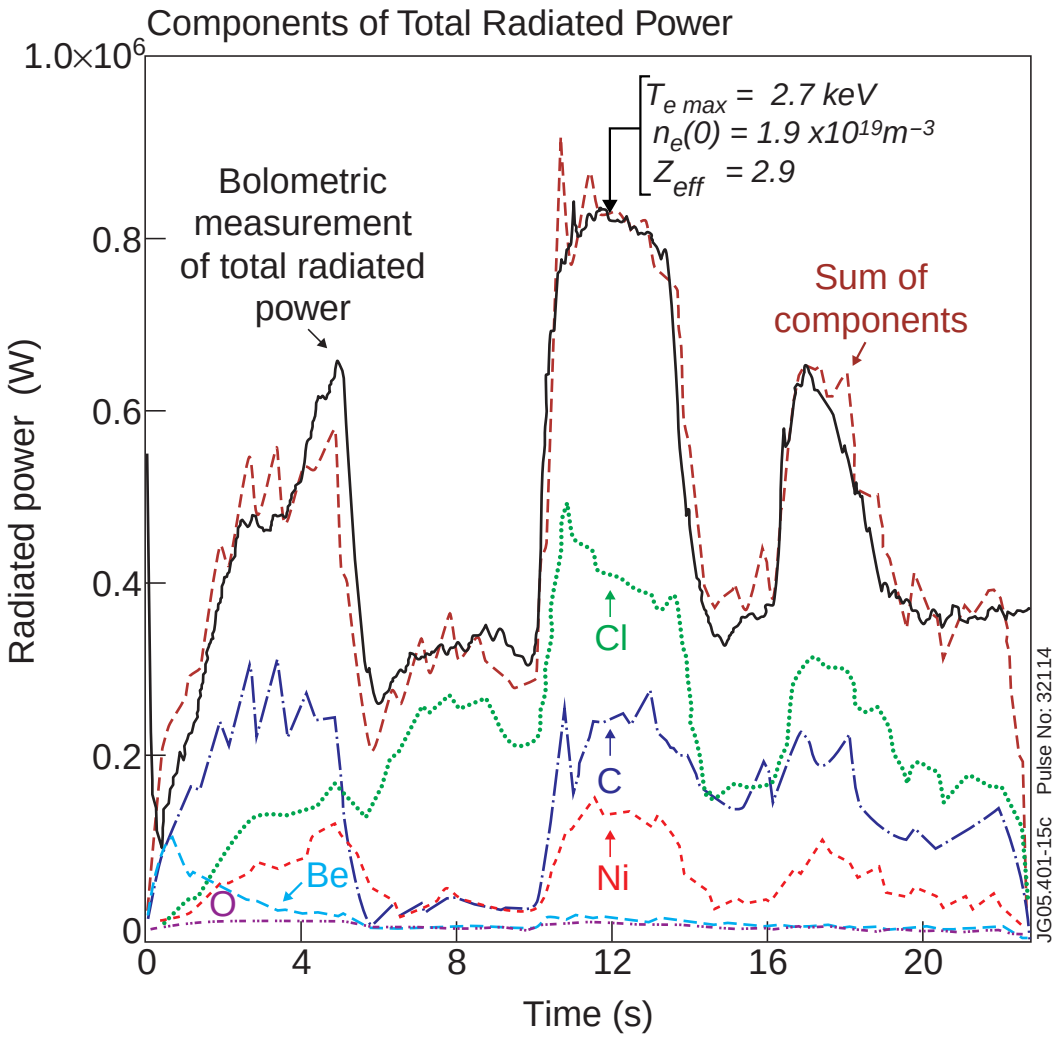

Pulse #32114 is a conditioning reference pulse in which the outer scrape-off plasma, initially in contact with the outer limiter, is moved progressively into an X-point phase followed by periods in contact with the external then the internal limiter and finally the outer limiter. The upward excursions in the total radiation correlate with increases in Zeff and correspond to plasma contact with the outer limiter.

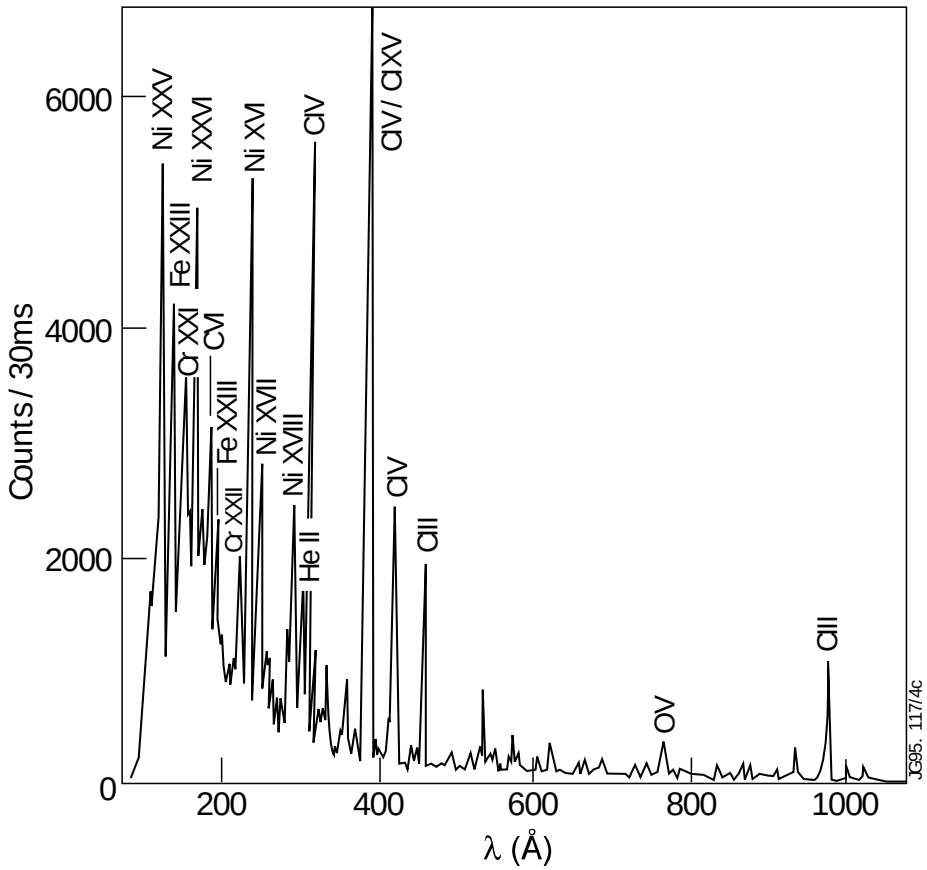

Horizontal LOS on JET indicates highly ionised metals.

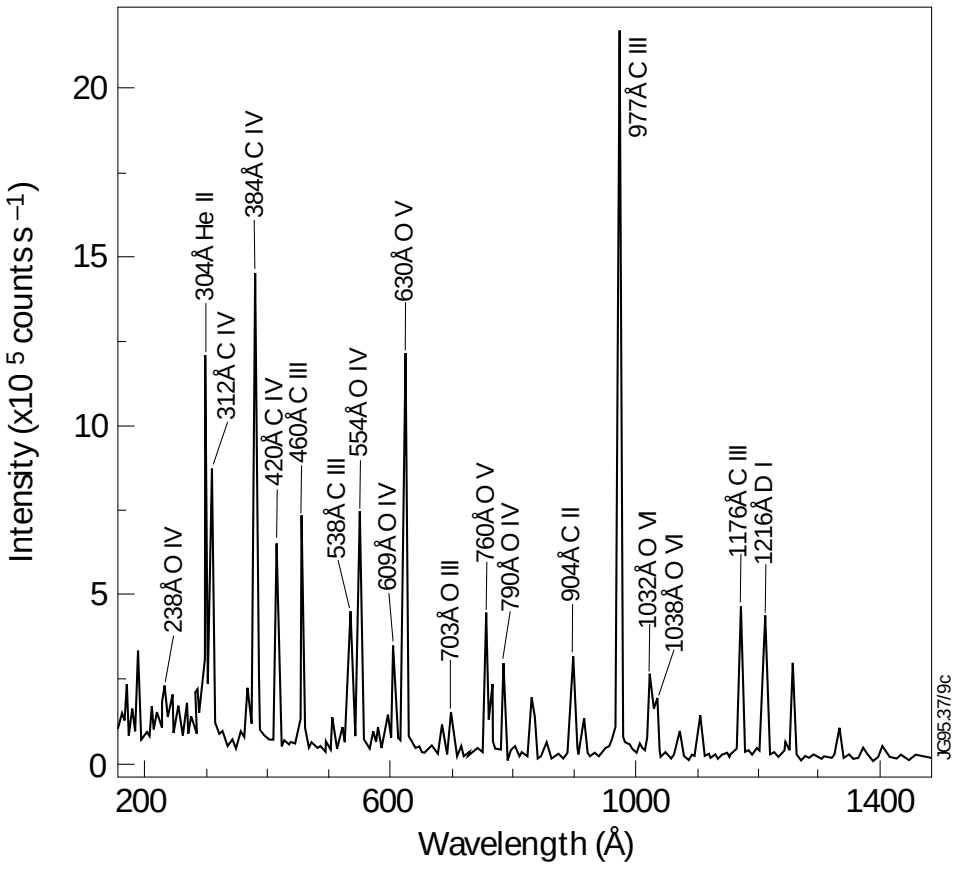

Vertical LOS through Divertor region on JET is dominated by lowly charged ions.

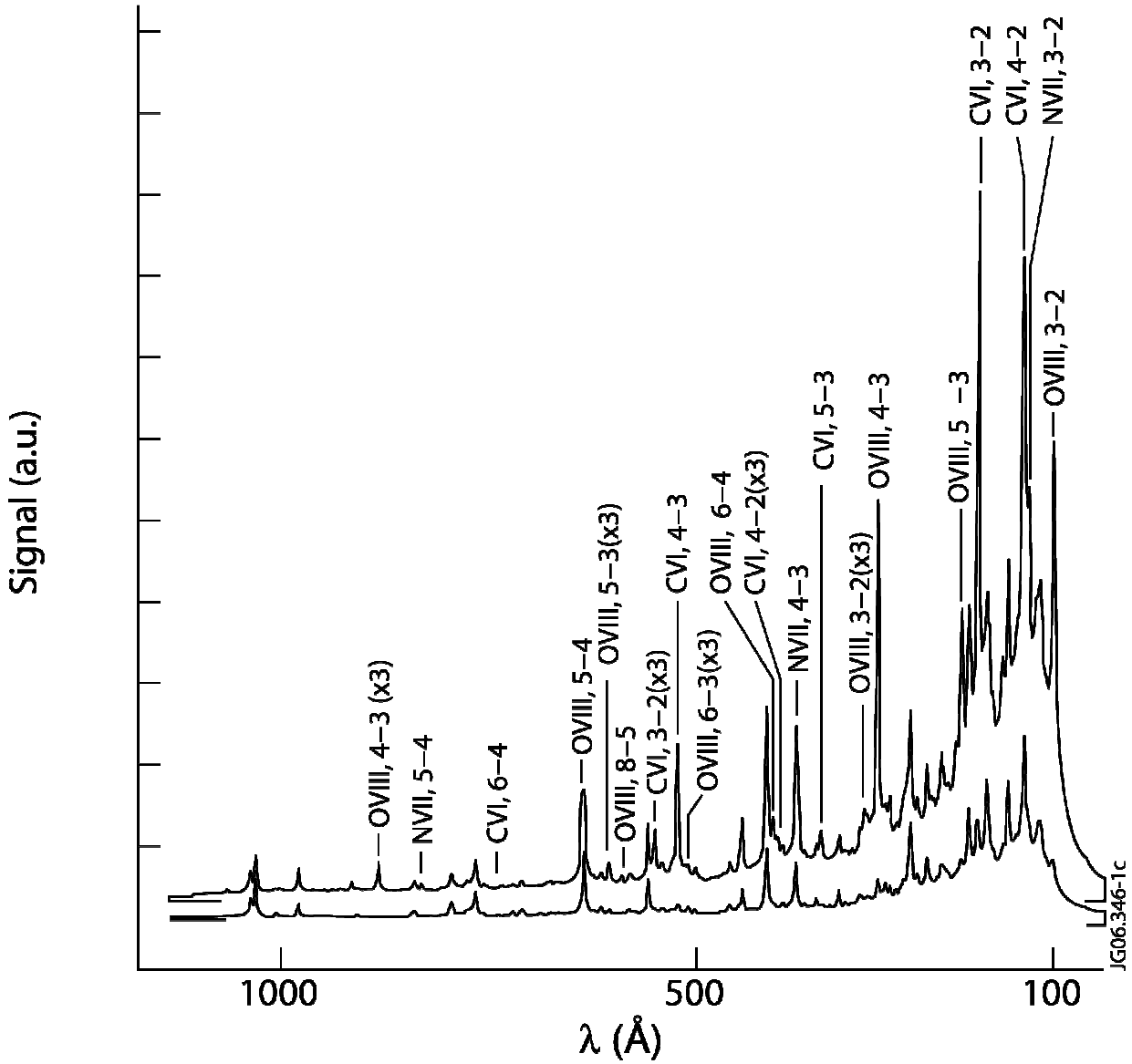

The VUV spectrum at two different times during an ASDEX discharge. The upper spectrum is taken at 1.370s during beam injection. The lower spectrum is at 1.40s just after beam switch-off . Exposure times are 16ms. All features annotated are CX lines in H-like ions and are present only during atomic beam injection.

Charge-exchange recombination spectroscopy gives **local** measurement
Based on charge exchange between heating neutral beam and fully stripped impurity ions. eg $D + C^{6+} \rightarrow D^{+} + C^{5+*} \rightarrow C^{5+} + h\nu$
Line width → Ion temp. **Line shift** → plasma motions. **Intensity** → impurity concentrations

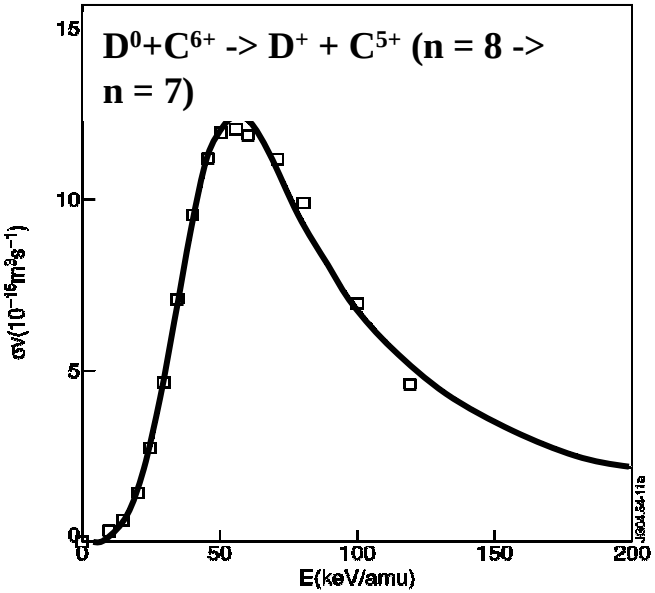

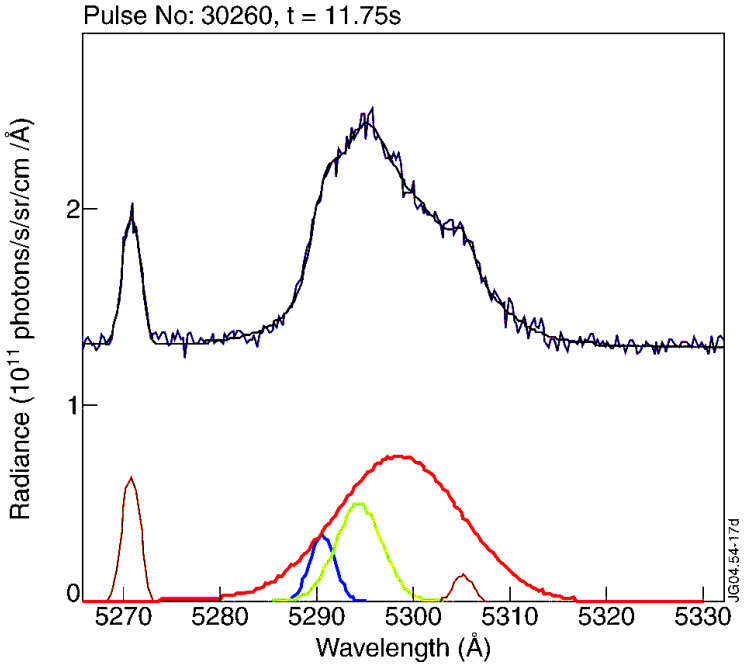

Peak CX cross-section is around 60 keV – typical of heating beams on current machines.
ITER has 1 MeV heating beams, and requires a diagnostic neutral beam for CXRS

Above: Measured spectrum, Fitted spectrum
Below: C^{5+} CX from Deuterium heating beam.
Electron impact excitation of C^{5+} in edge plasma.
C^{5+} CX from edge neutrals.
Background lines Be^{+} 5271 & C^{2+} 5305

Example of the use of Charge Exchange measurements on JET

Internal transport barrier **#51976**

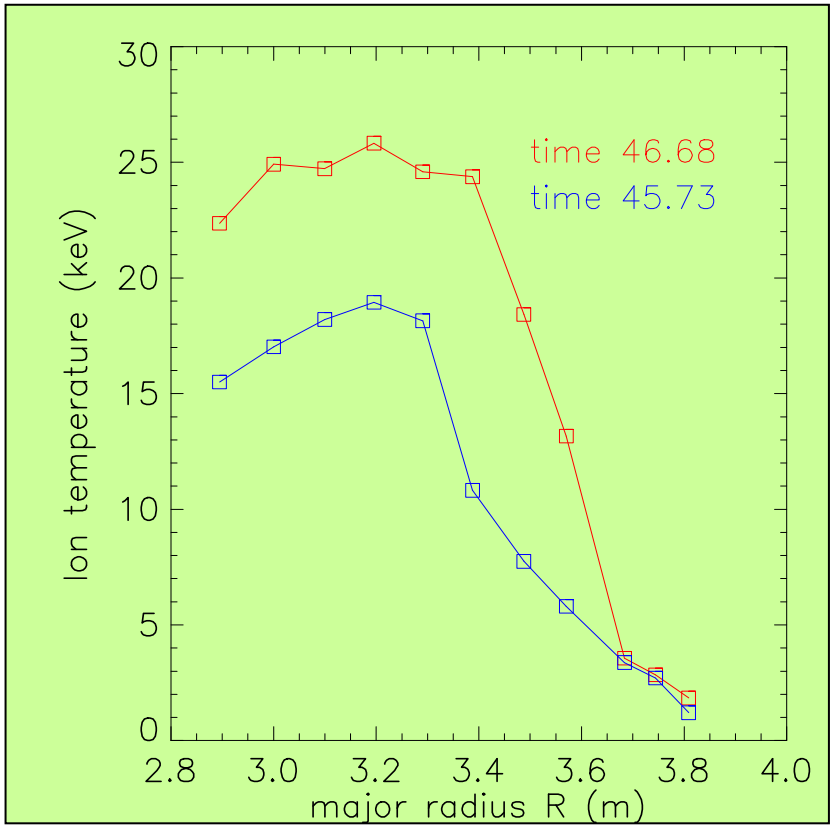

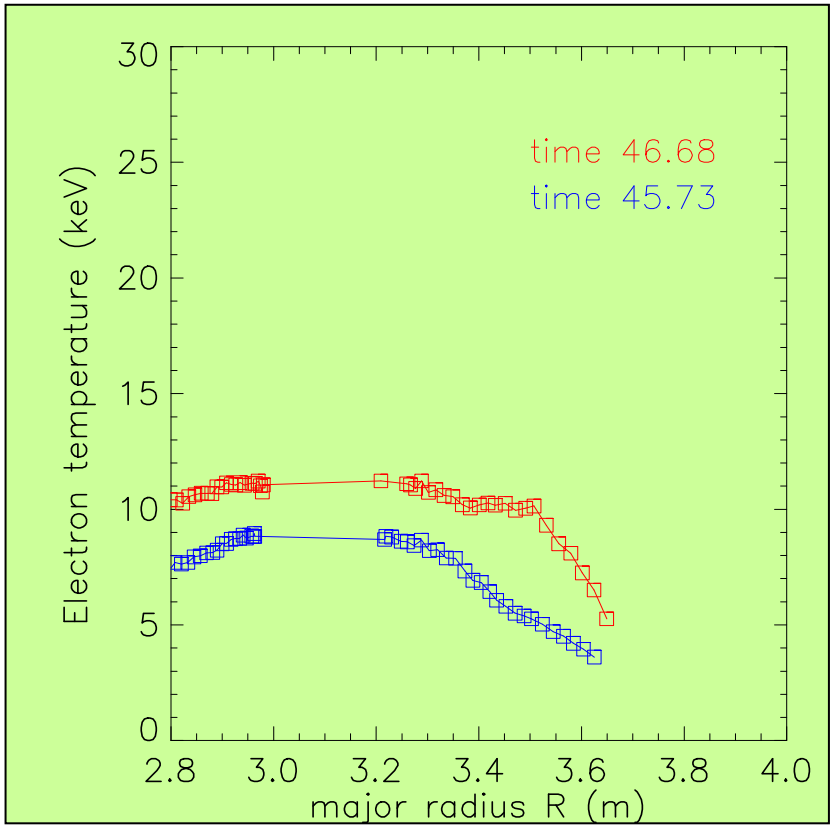

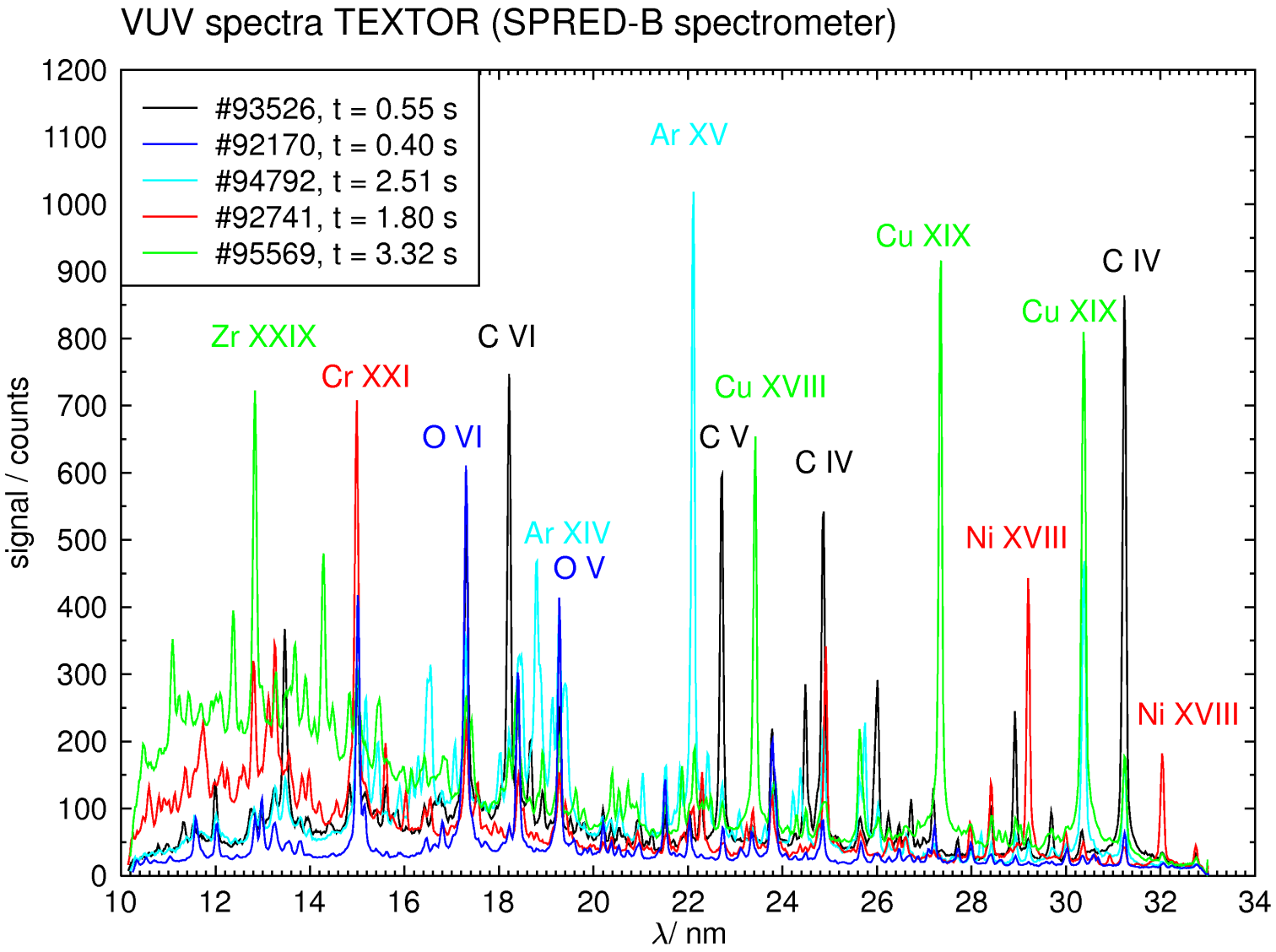
VUV spectra TEXTOR (SPRED-B spectrometer)
#93526, t = 0.55 s
#92170, t = 0.40 s
#94792, t = 2.51 s
#92741, t = 1.80 s
#95569, t = 3.32 s
Zr XXIX
Cr XXI
O VI
C VI
Ar XIV
O V
Ar XV
C V
Cu XVIII
C IV
Cu XIX
Ni XVIII
Cu XIX
C IV
Ni XVIII
signal / counts
λ/ nm
0
100
200
300
400
500
600
700
800
900
1000
1100
1200
10
12
14
16
18
20
22
24
26
28
30
32
34

Spectroscopic approach to diagnosis of impurity emission from ITER using array of x-ray detectors with 5% band-pass over the energy range 0.1-100keV.

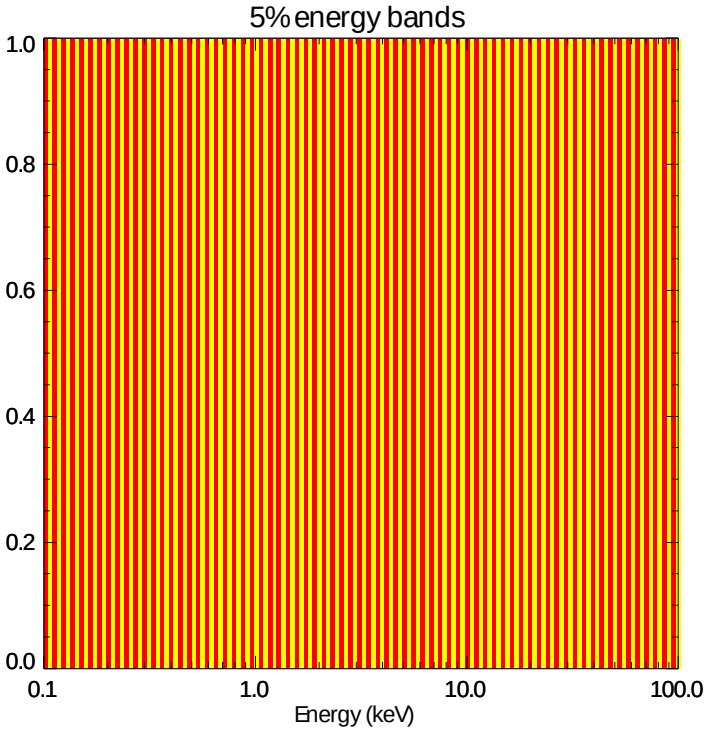

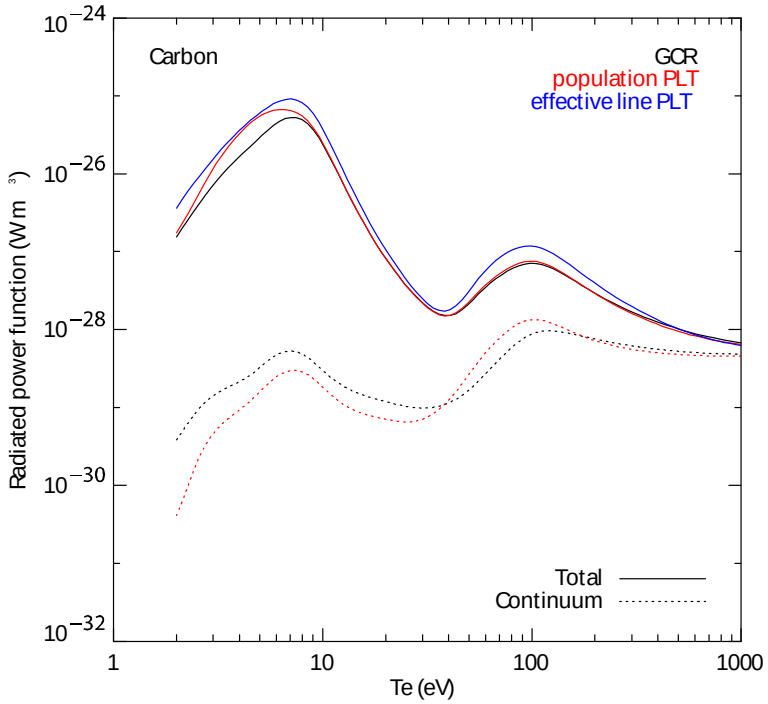

ADAS uses Generalised Collisional radiative (**GCR**) model (in detail for Z ≤ 10) but framework includes other density dependent methods e.g. **Population PLT** for calculating total line power. **Effective Line Population (PLT)** is density independent and assumes total line power approximates to a few lines connected to the ground state (not used yet for W). Comparison above refers to carbon equilibrium balance at n_e = 10^{19} m^{-3}.

ITER scenario #2 15MA, 400MW fusion power for ~400s.

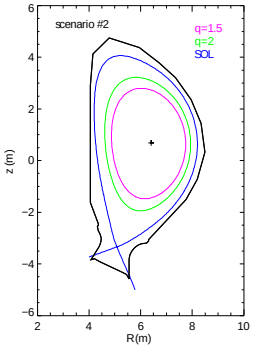

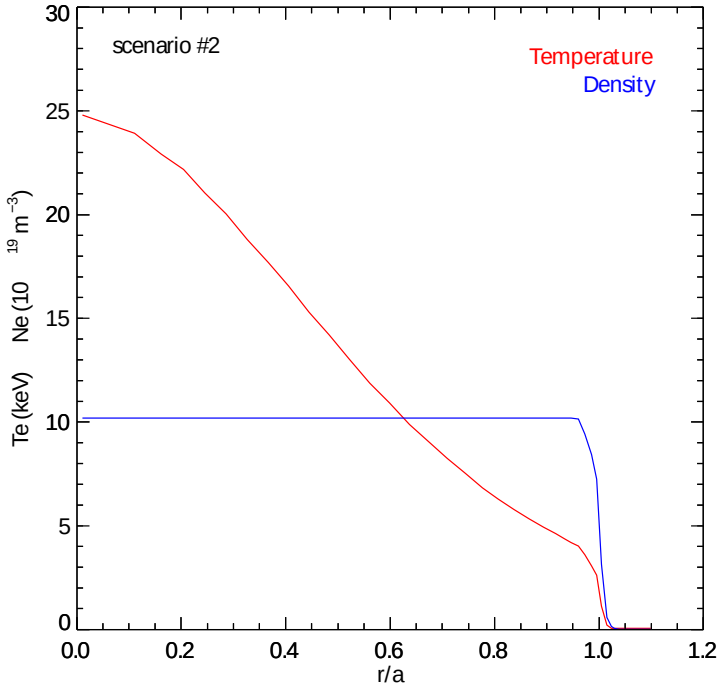

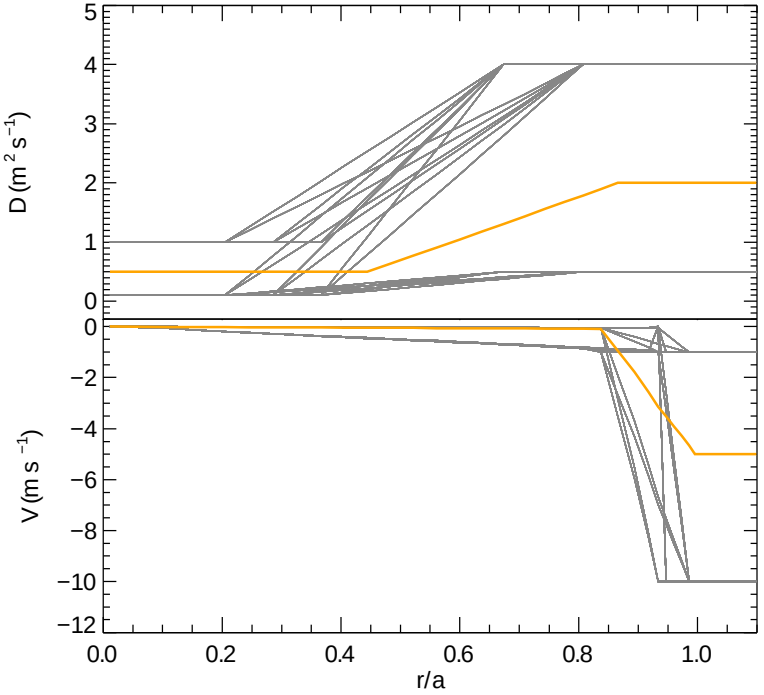

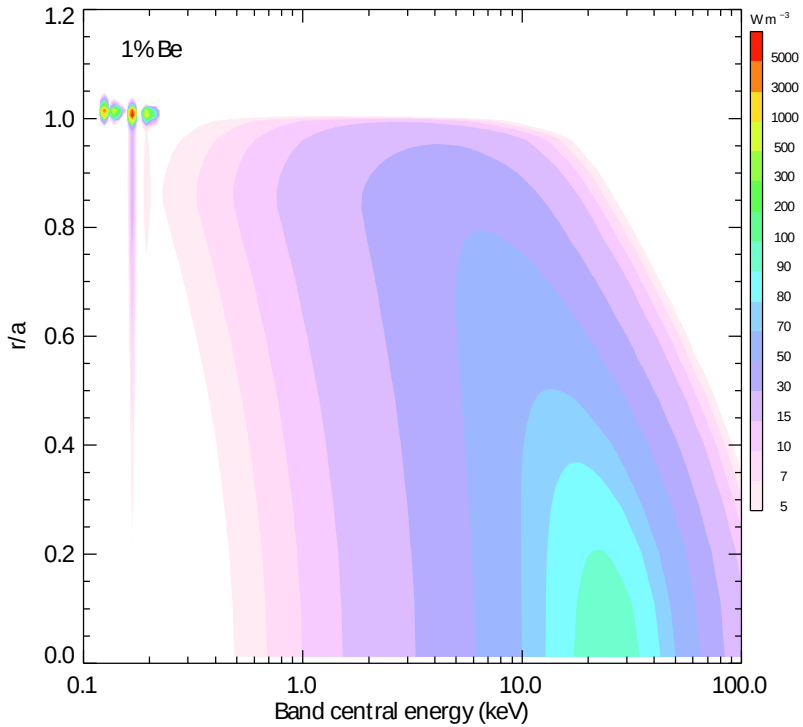

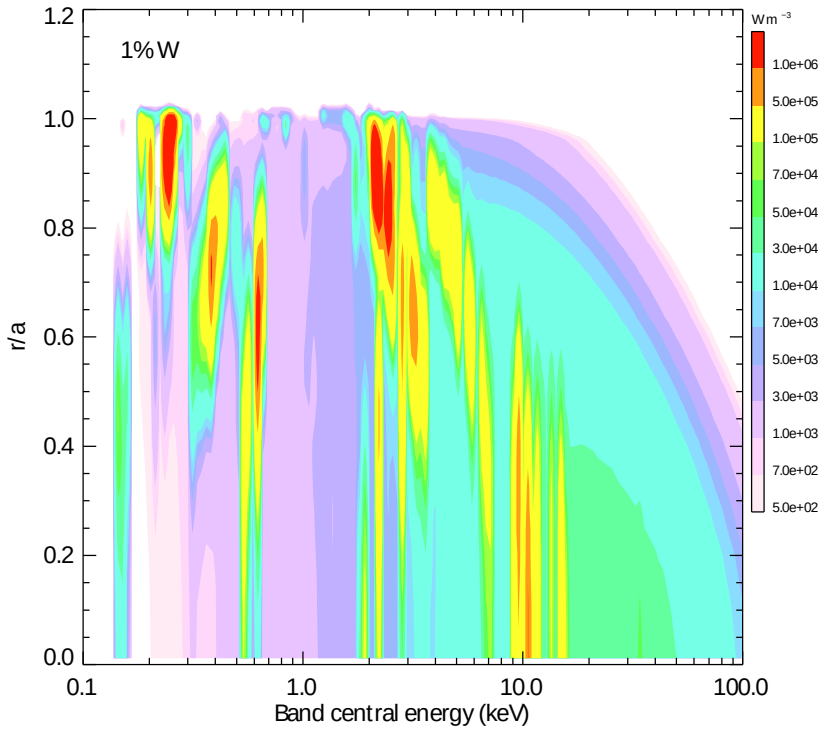

X-ray emission for 1% impurity In ITER (scenario #2) plasma.

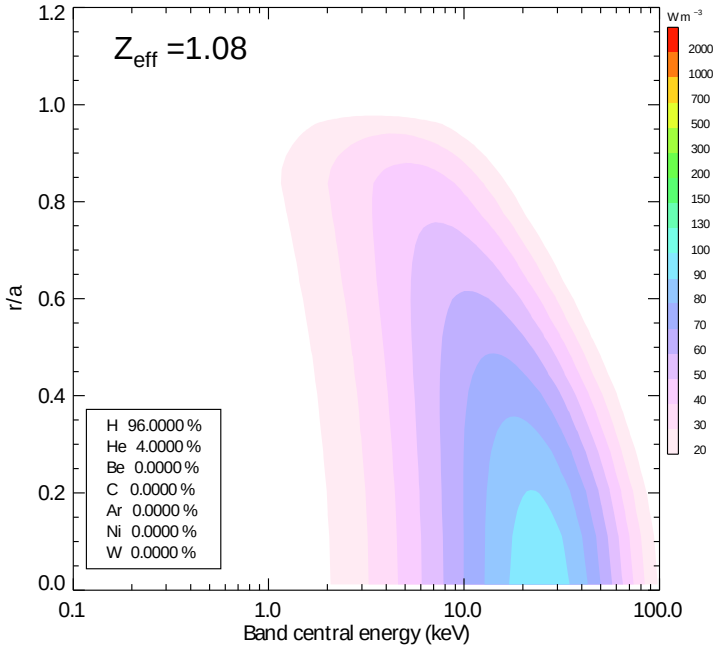

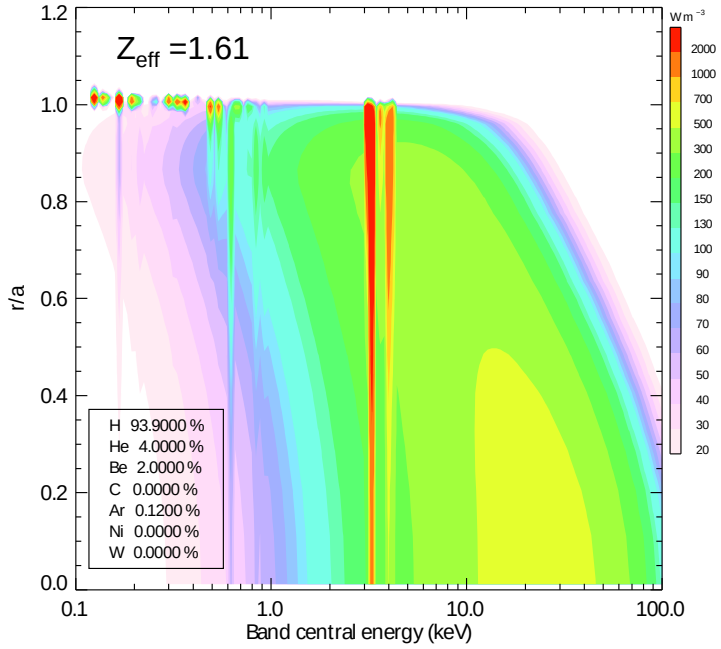

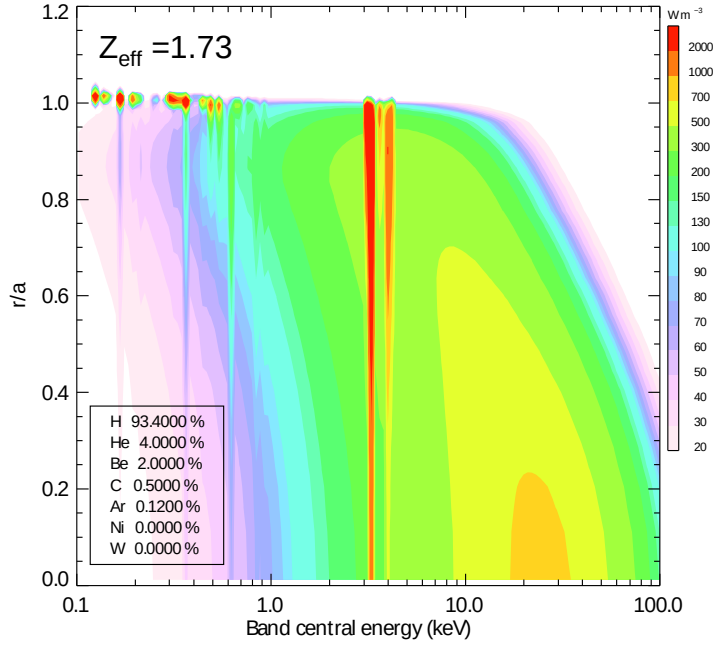

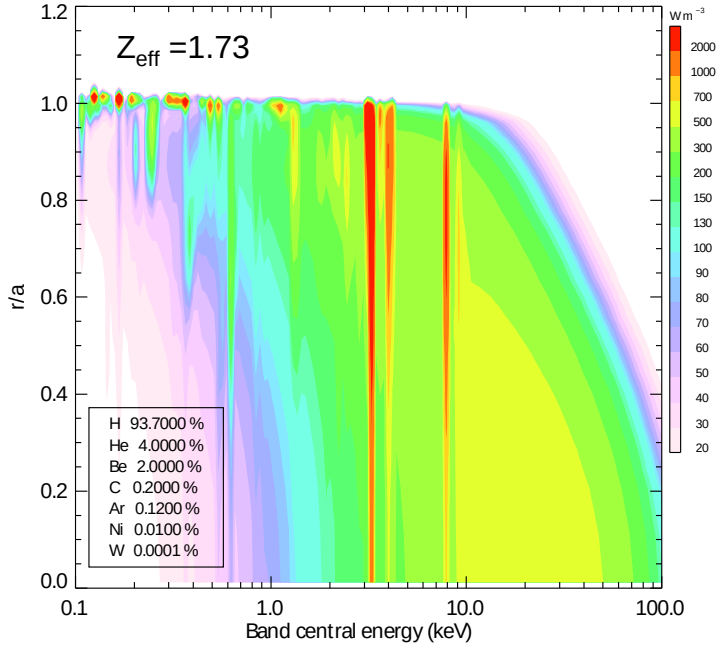

Composite X-ray emission for impurity mixes: Z_{eff} =1.08) 1.61) 1.73) 1.73)

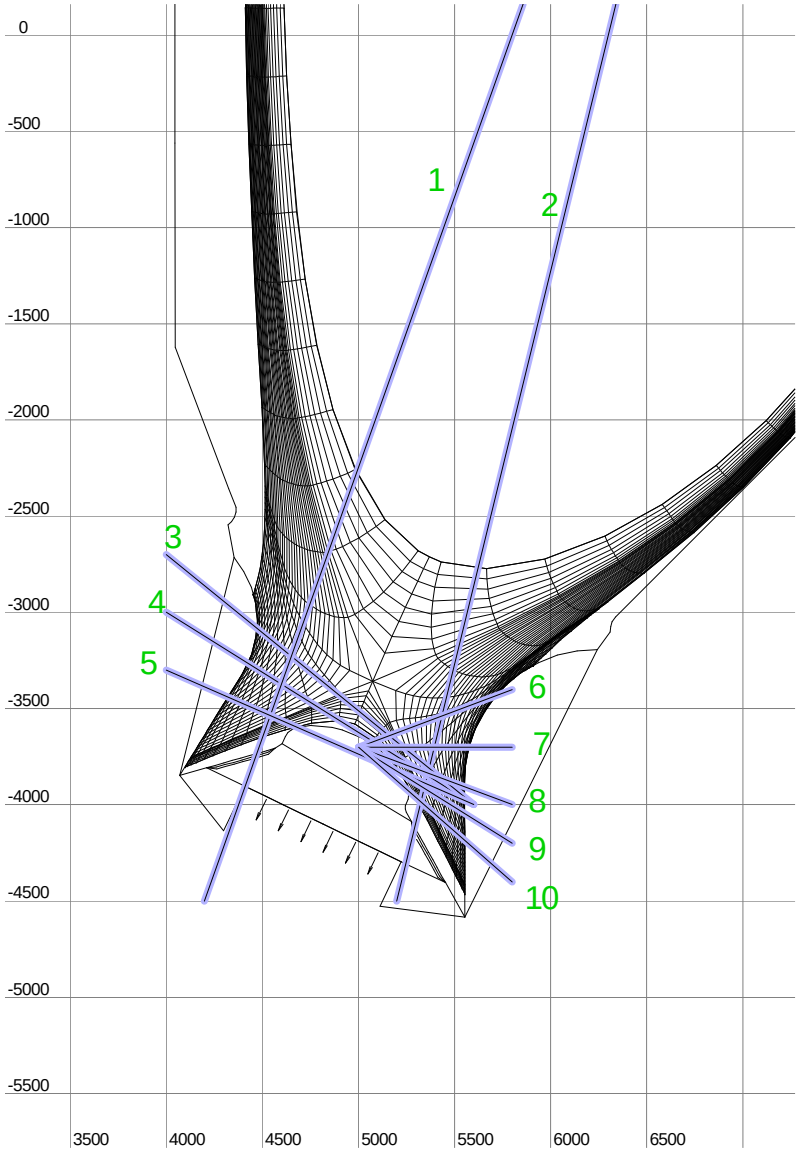

Line Of Sights (LOS) used in analyses of spectral signature from divertor region in ITER. Standard ITER H-mode plasma core parameters were matched to B2-Eirene simulations of the divertor/edge plasmas. He Be C Fe and W(10^{-4} n_e) impurity mixes chosen with $1.5 \leq Z_{eff} \geq 2.5$.

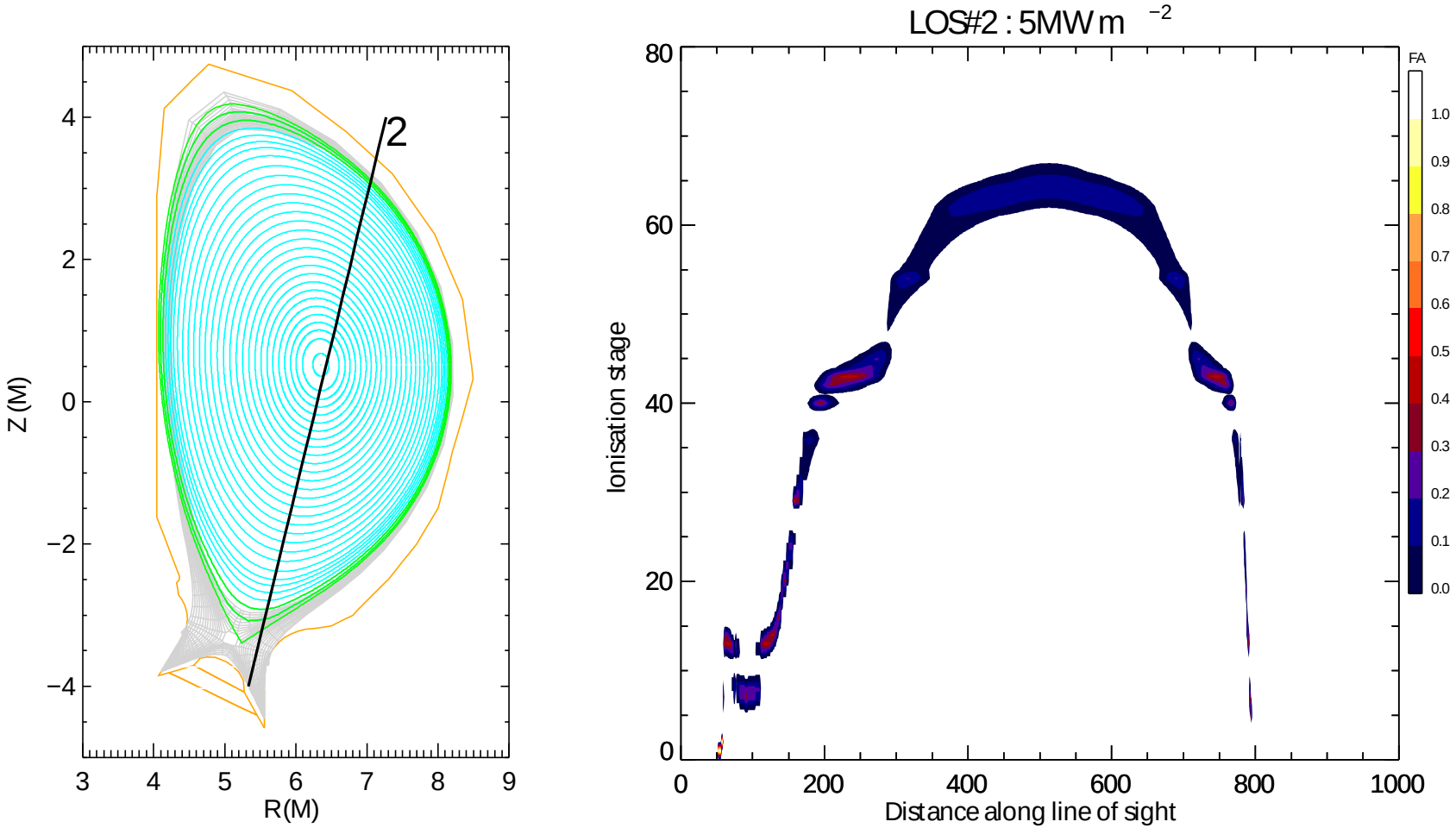

Tungsten ionisation balance along LOS # 2. **W^{60+}** (Si-like) is highest ion stage accessed.

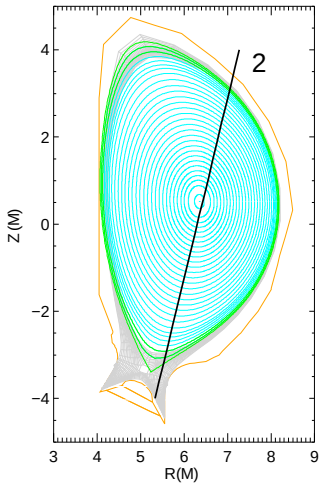

Spectral radiance along LOS # 2 with different impurity mixes. Edge region excluded. No Tungsten.

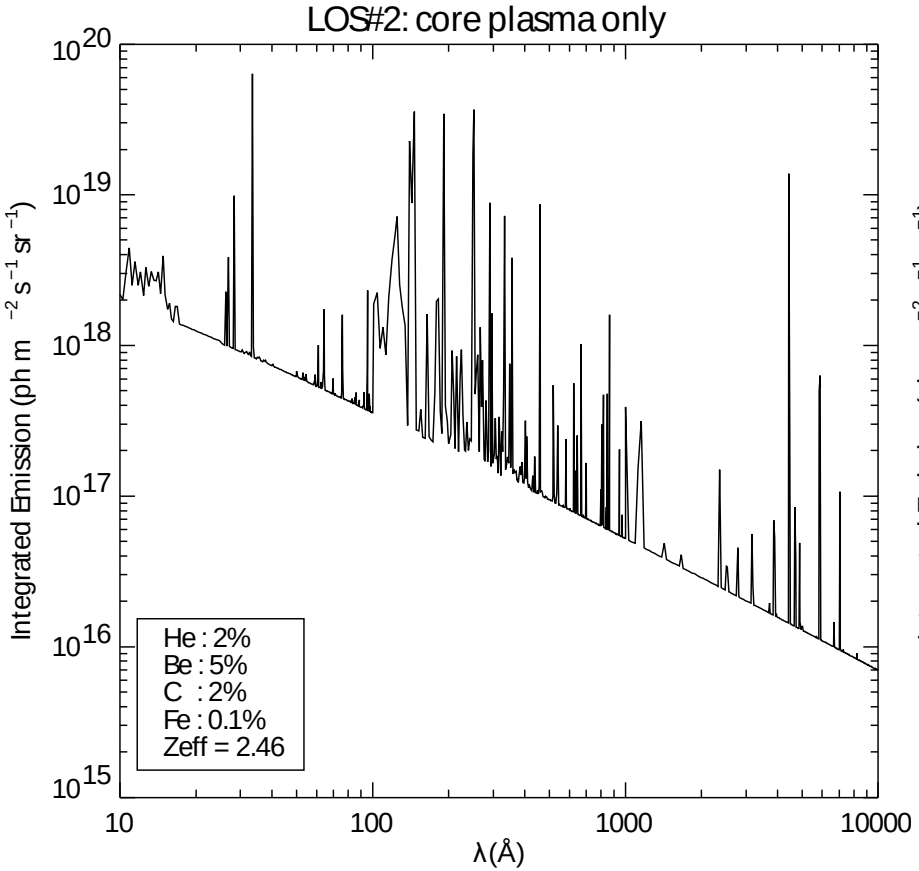

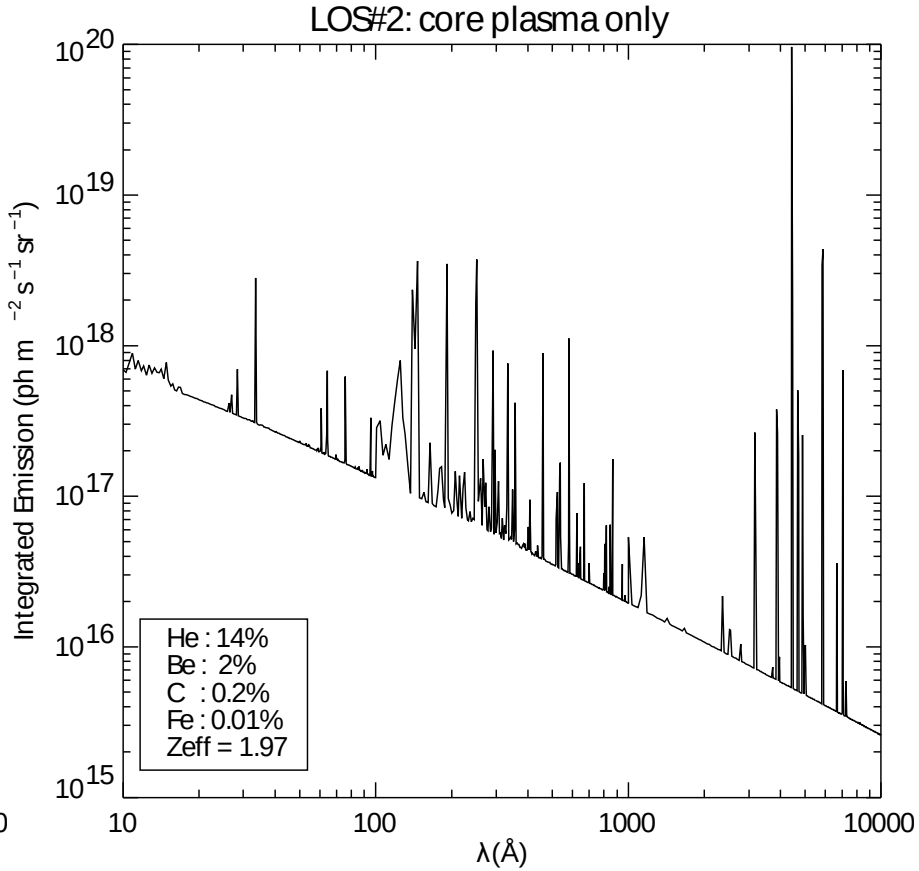

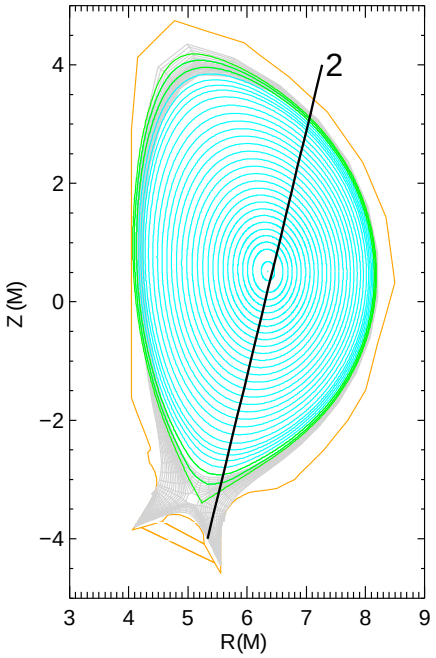
2
Z (M)
R(M)
4
2
0
−2
−4
3
4
5
6
7
8
9

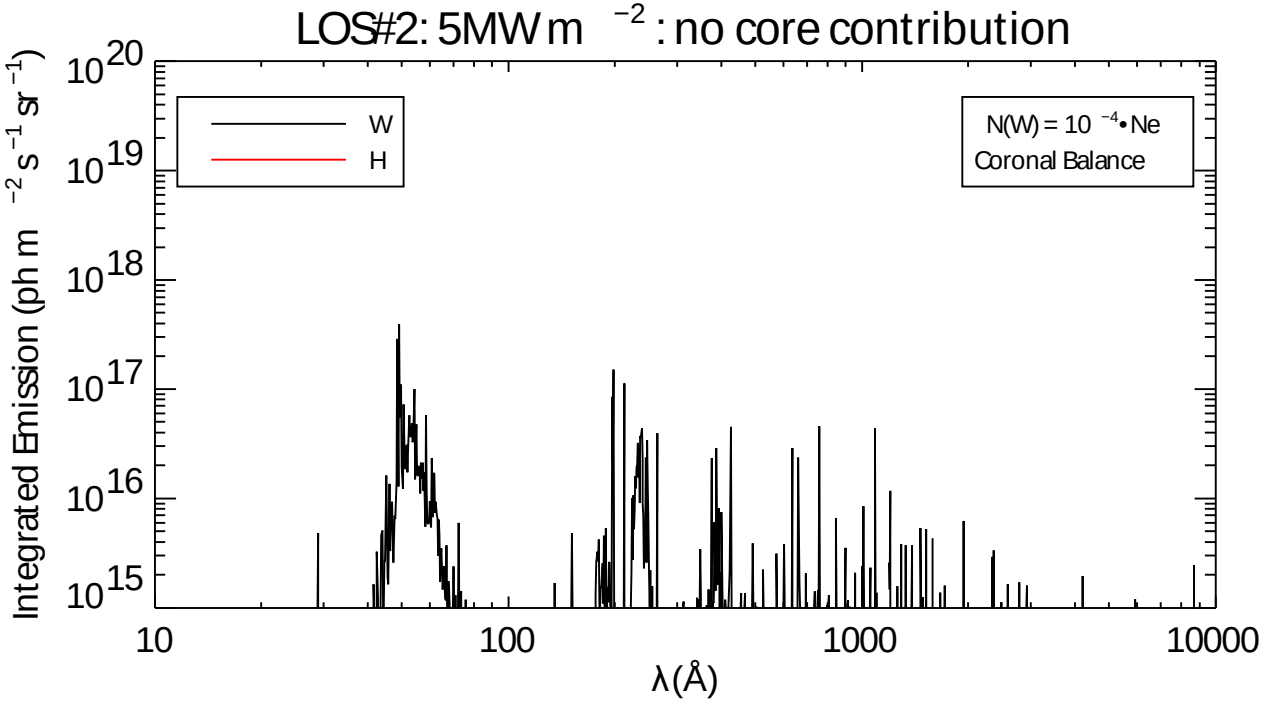
LOS#2: 5MW m −2 : no core contribution
Integrated Emission (ph m −2 s −1 sr −1)
λ(Å)
W
H
N(W) = 10 −4 • Ne
Coronal Balance
10 20
10 19
10 18
10 17
10 16
10 15
10
100
1000
10000

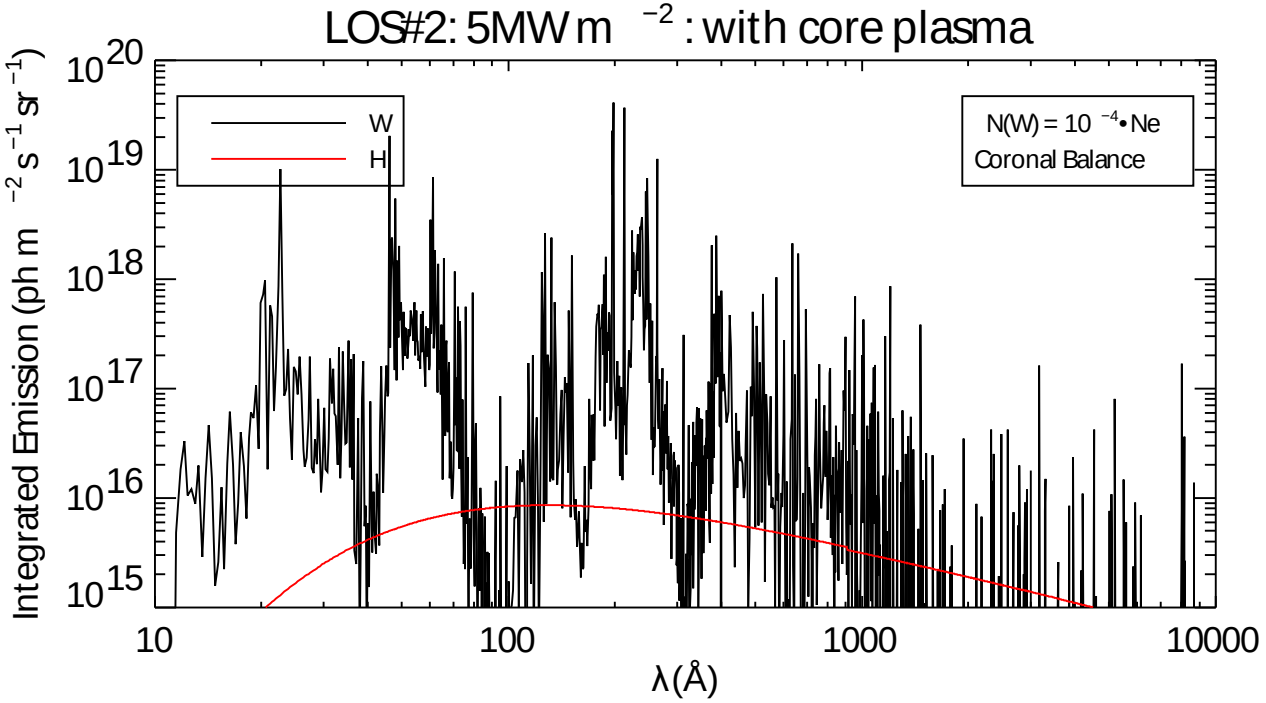
LOS#2: 5MW m −2 : with core plasma
Integrated Emission (ph m −2 s −1 sr −1)
λ(Å)
W
H
N(W) = 10 −4 • Ne
Coronal Balance
10 20
10 19
10 18
10 17
10 16
10 15
10
100
1000
10000

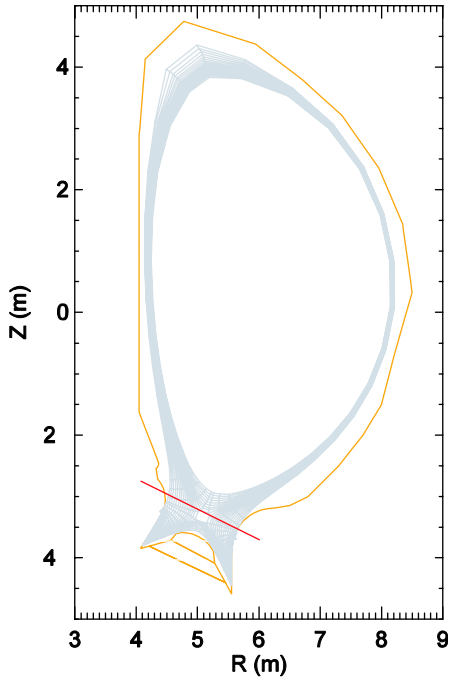

Modeled Tungsten spectrum in ITER divertor

Left Modeled divertor sight-line

Right Line excitation coefficients indicate spectra (100-400 Å) from individual W ionization stages: W^{6+} → W^{20+}

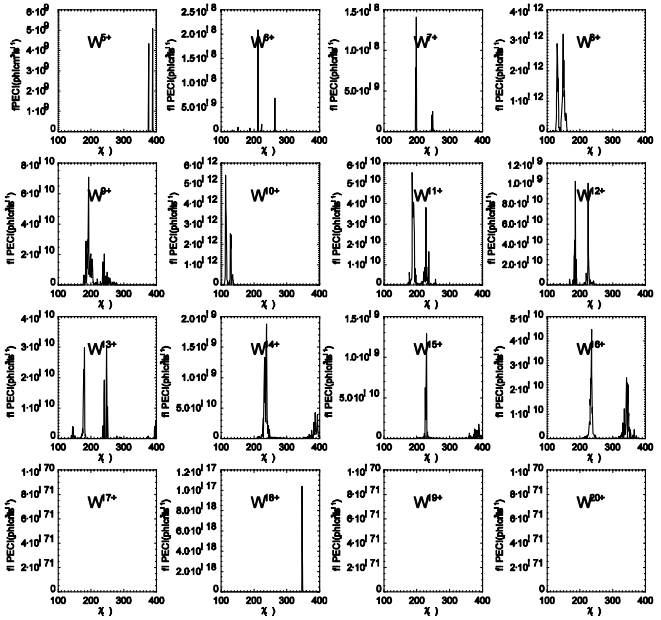

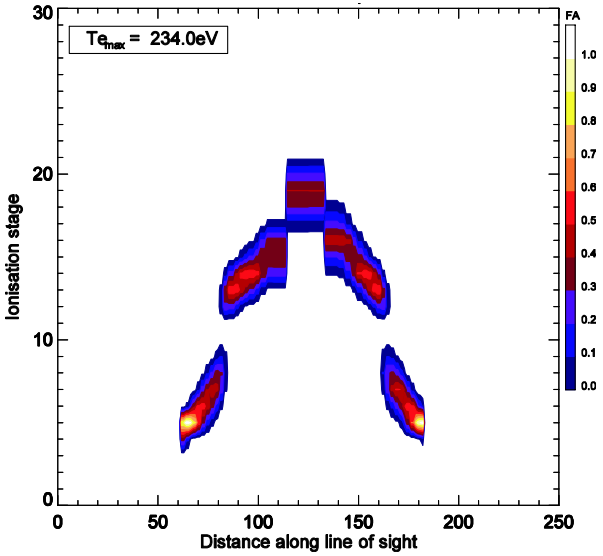

Left W ionization balance along divertor sight-line

Right Composite **W** spectrum along LOS.

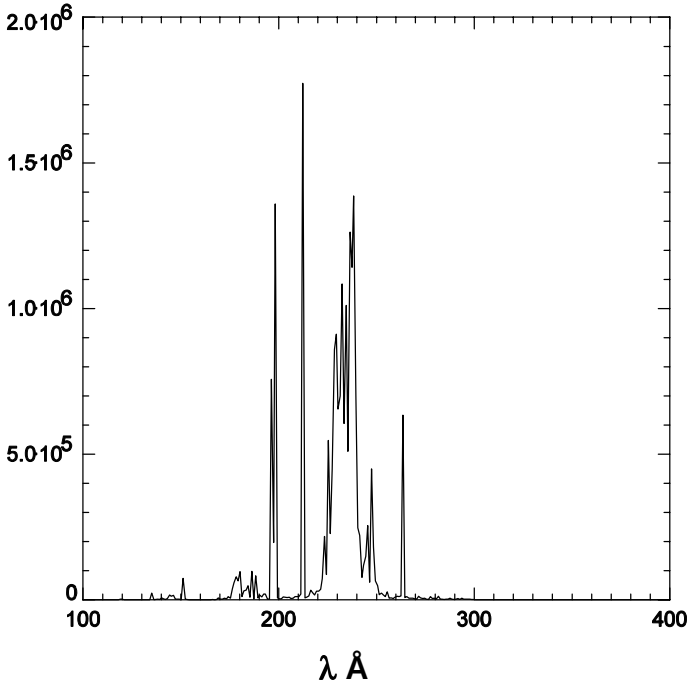

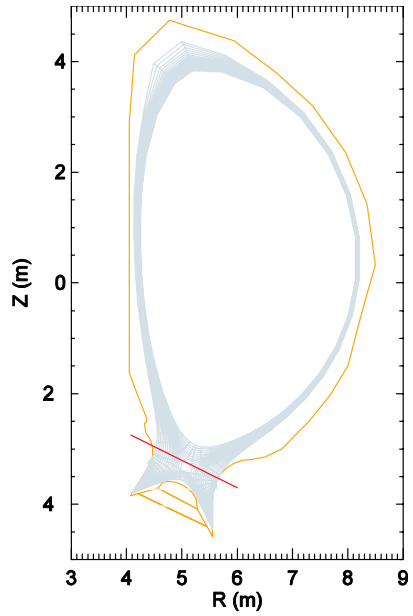

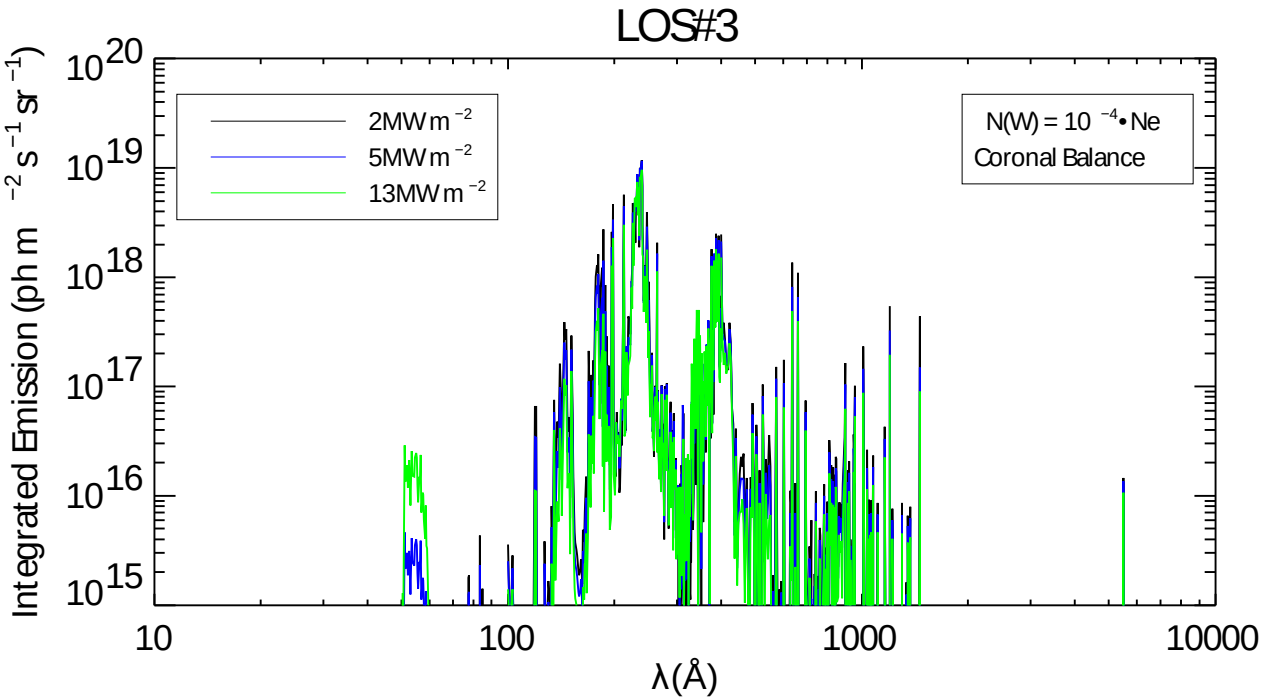

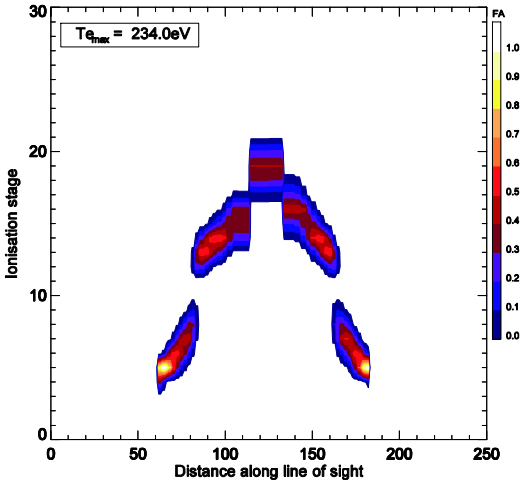

Integrated emission from Tungsten with concentration of 10^{-4} x n_e under different power loadings on the divertor. Note that W emission features from divertor lie at λ > 40 Å.

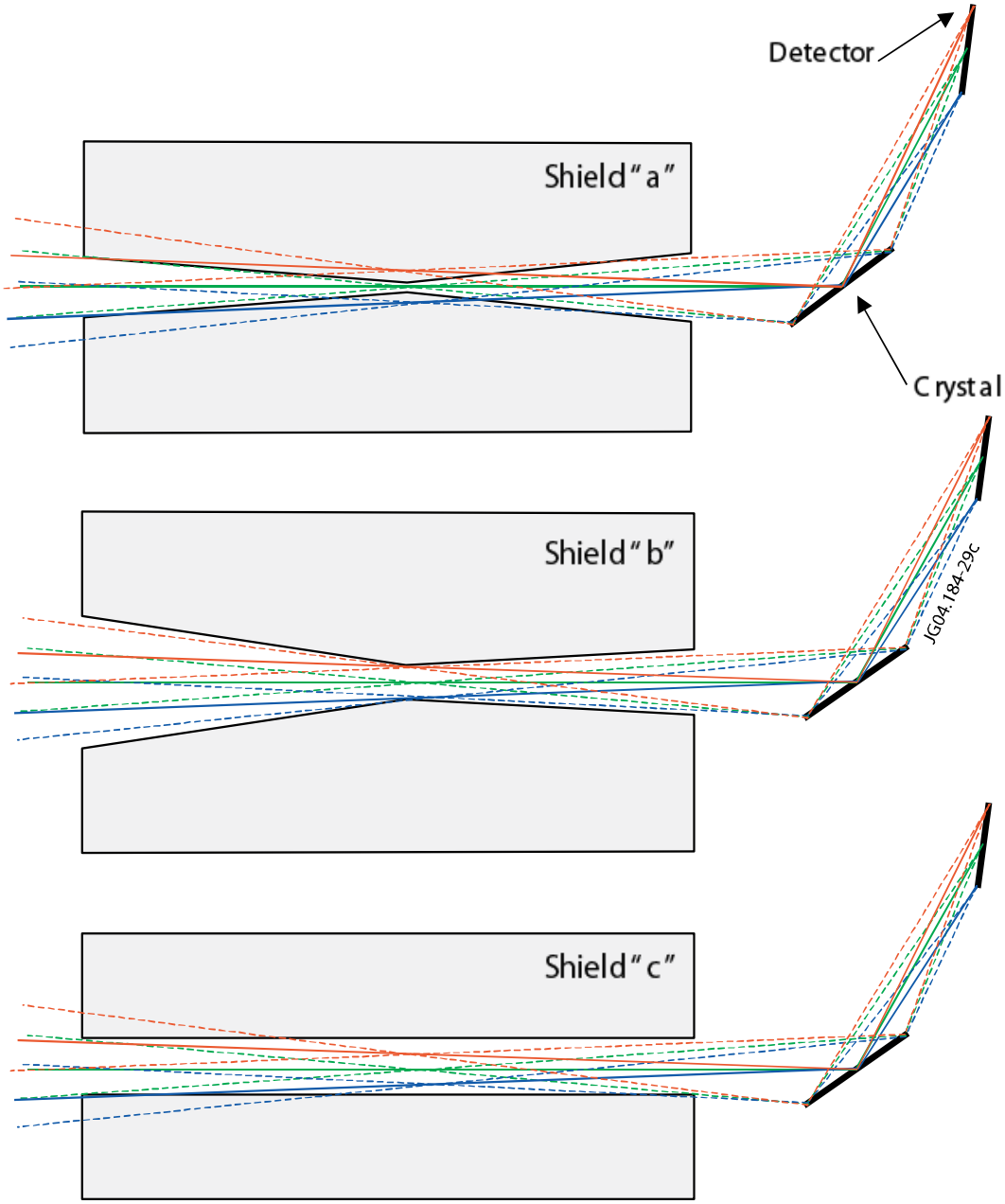
Detector
Shield "a"
Crystal
Shield "b"
JG04.184-29c
Shield "c"

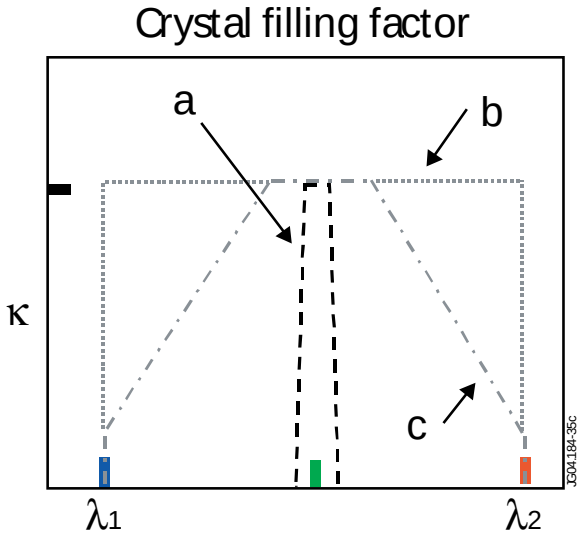
Crystal filling factor
a
b
c
κ
λ1
λ2
JG04.184-35c

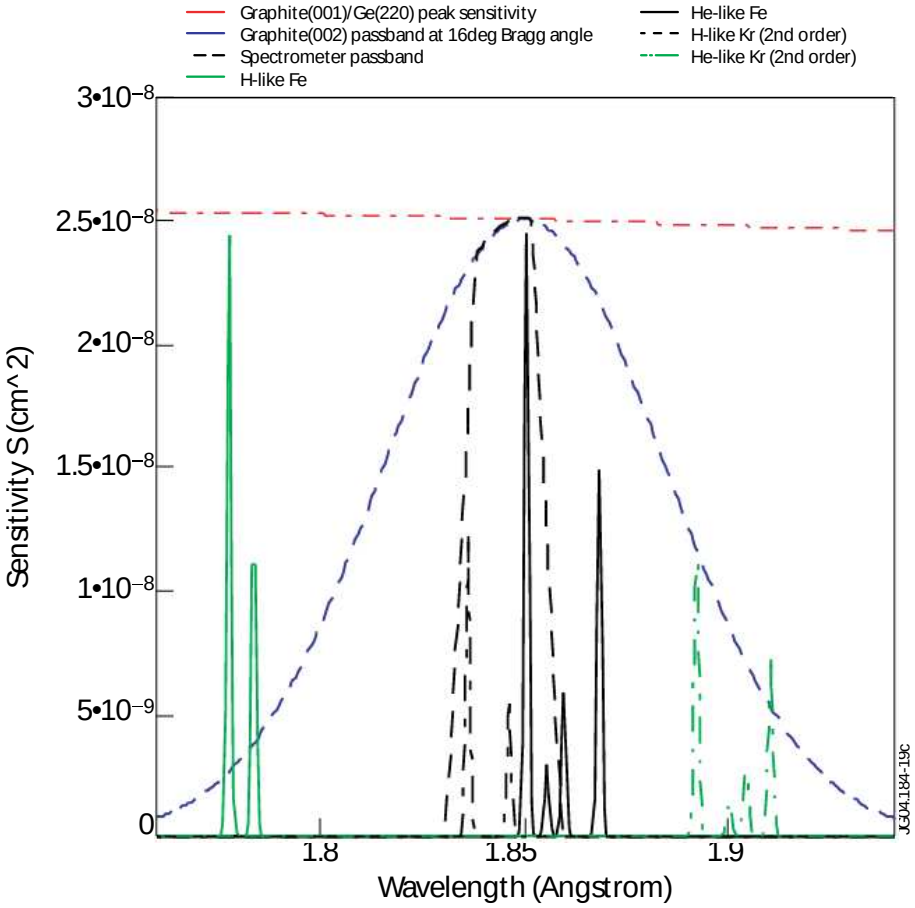

Spectrometer pass-band in the region of the principal lines of H- and He-like Fe and Kr for a Johann spectrometer with graphite pre-reflector.

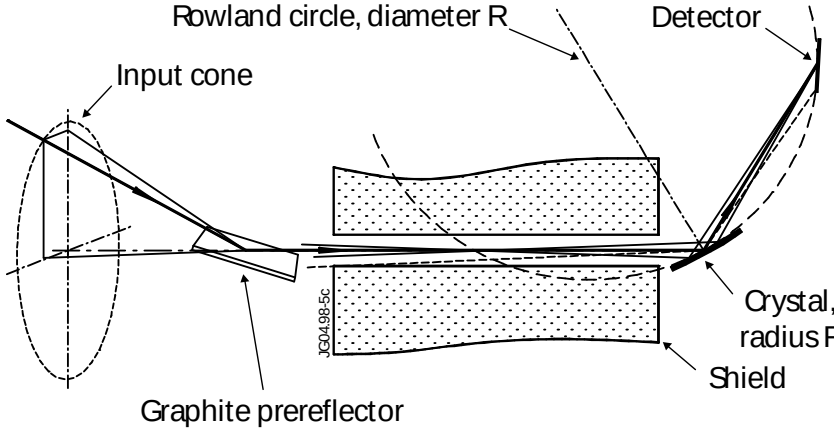

Schematic of Johann spectrometer with graphite pre-reflector allowing toroidal and poloidal LOS's. Viewing aperture determines $\Delta\lambda$ and crystal filling factor.

Modeled neutron levels for the ITER upper port imaging crystal spectrometer.

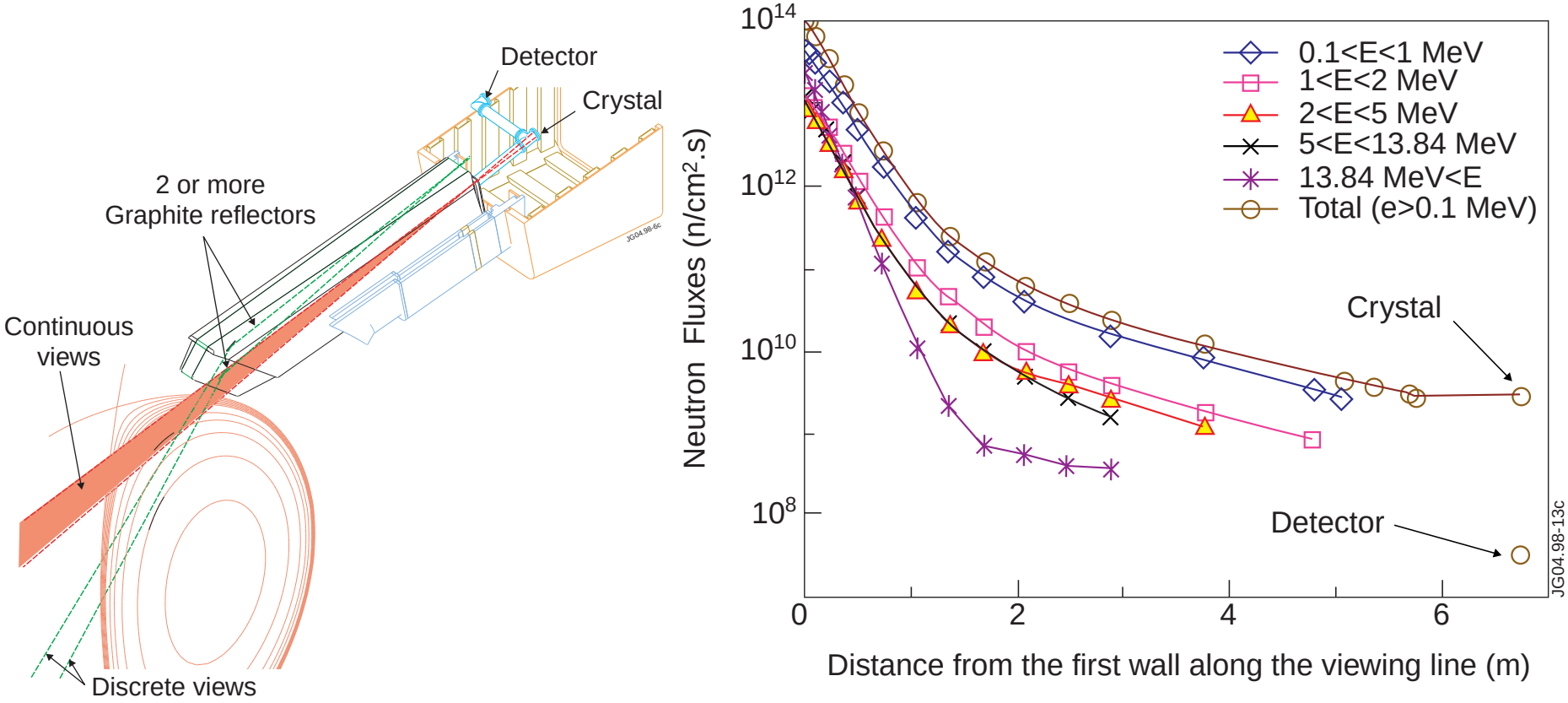

Neutron flux behind port-plug is manageable, and detector replacement is possible

Remoteness from plasma usually results in lost sensitivity, bandwidth, etc.

Reference designs are based on current technology

Increased radiation hardness of detectors would allow closer approach to plasma

Performance of SPRED spectrometer on JET during DT pulses.

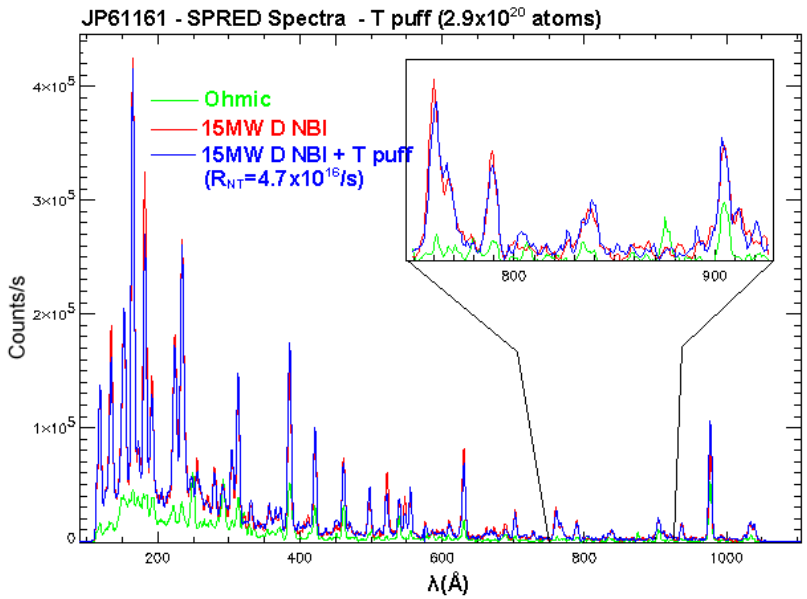

- Tritium was injected either by neutral beams or gas puffing.
- The TTE produced a total neutron yield of $4x10^{18}$ 14MeV and $5.5x10^{18}$ 2.45MeV neutrons and introduced ~ 380mg of tritium by gas puffing.
- The SPRED spectrum is shown during tritium beam injection and tritium gas puffing pulses. There is no discernible increase in the noise levels in either case. The tritium injection pulse shown had the highest peak neutron yield of the TTE campaign

Comparison of estimated direct neutron fluxes for JET and ITER spectrometers. For scattering into detectors, the total influx into the spectrometer is relevant. For neutron damage to crystals and mirrors, the neutron fluence is relevant.

System	Shielding option	Etendue **/JET.**	Neutron influx into Instrument **(10^9/s).**	Neutron flux at xtal **(10^9/cm^2.s)**	Neutrons into inst. **/JET.**	Neutron flux at xtal **/JET**.
JET VUV/XUV beamline		1	0.7	0.008	1	1
JET High Resolution Xtal	Partial spectrum Bandwidth ~ 0.5 %		0.8	0.017		
ITER equatorial X-ray imaging Array. (3-5 Spectrometers/array Two arrays required to isolate V_{pol} from V_{tor})	Full spectrum bandwidth ~ 1%	6.8	28	1.1	40	140
	Single line Bandwidth ~ 0.25%	2.3	7	0.3	10	35
	Single line Reduced sensitivity→0.1	0.17	0.7	0.3	1	3.5
ITER Equatorial X-ray survey		0.17	0.7	0.03	1	3.5
ITER Equatorial XUV-VUV survey		0.17	0.7	0.03	1	3.5
ITER upper port X-ray imaging	Full spectrum Bandwidth ~1%	5.4	22	0.9	31	110

Design for ITER imaging x-ray crystal spectrometers

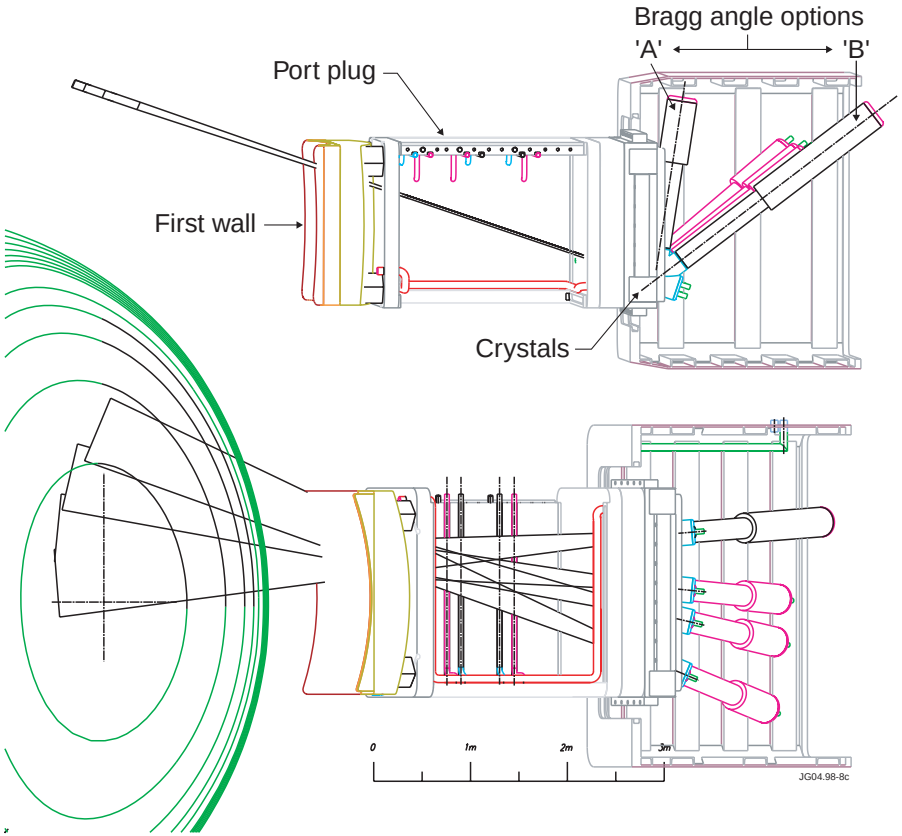

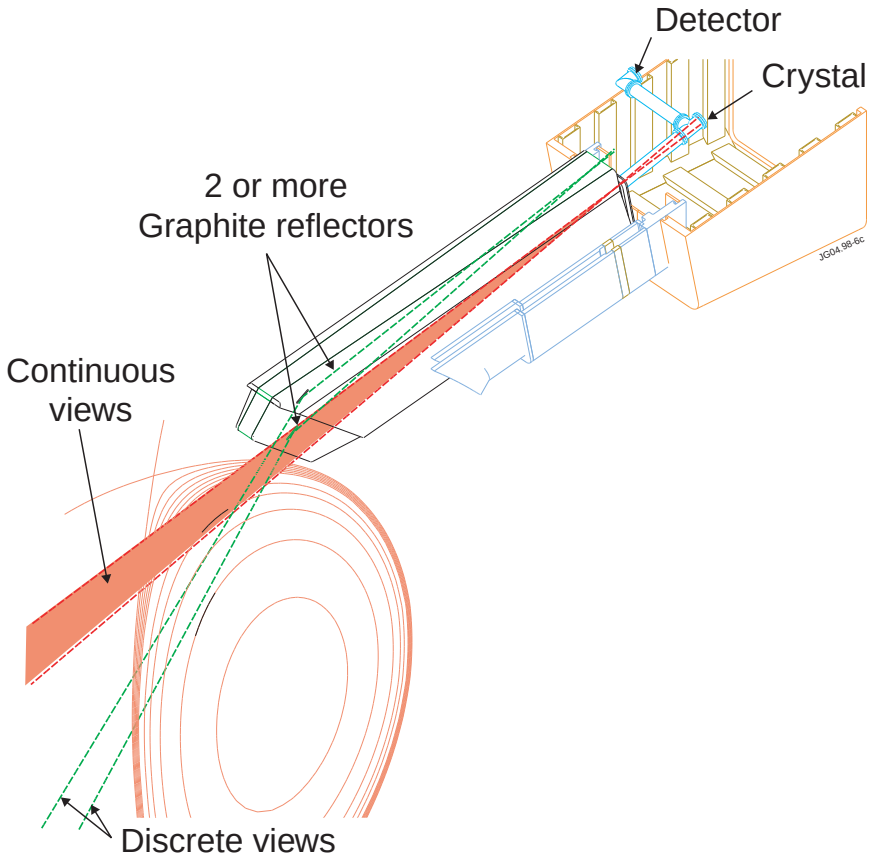

Equatorial port:options
"A": Spherical crystals - better optically
"B": Toroidal crystals - better S/N
~ 3m crystal radius:
- Could use gas or solid state detector

Upper port
Part of plasma cannot be viewed directly
- graphite reflectors are used.
- ~ 1m crystal radius
- Dispersion too low for gas detector,
ideal for solid-state pixel-detector

Role of EBIT

- **"Ground-based" (i.e. neutron damage –free) station which provides standards of emission coefficients and emission line profiles with which to monitor and evaluate ITER spectroscopic diagnostics. Polarisation corrections.**

- **Precision wavelengths and differences $\Delta\lambda$ from nearby wavelength standards such as absorption edges and characteristic diode lines. Small plasma rotational velocities ≥ 1 kms^{-1} derived using $\Delta\lambda$.**

- **Line identifications. At present, low $W^{+6} \rightarrow W^{+20}$ are of great interest.**

- **Charge exchange "distortions" to basic spectra due to collisions with ground and excited state (n=2) neutrals (from beams in ITER).**

- **Forbidden lines in high Z ions.**

* **Collision rate coefficients**

Signal-to-noise improvement with energy dispersive detector on Oxford EBIT

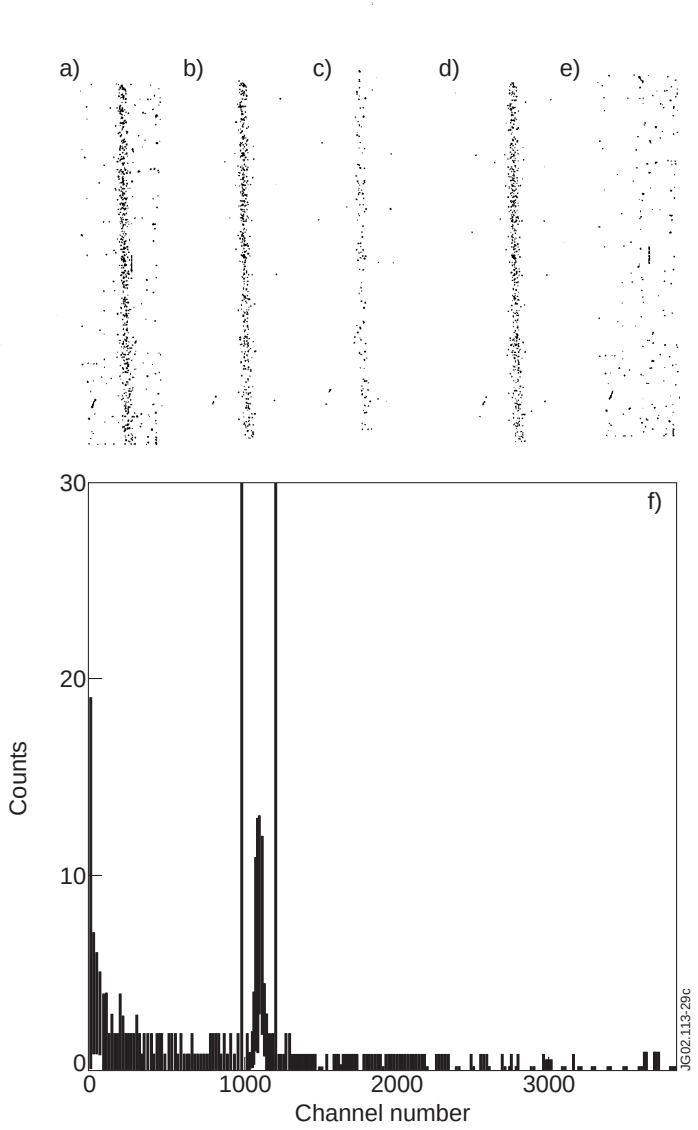

Left CCD image and energy spectrum
a) All events **b)** Spread events
c) Single pixel events
d) Counts in energy window (below left)
e) Removed counts
Below Resulting wavelength spectrum
Count-rate ~1 count/s

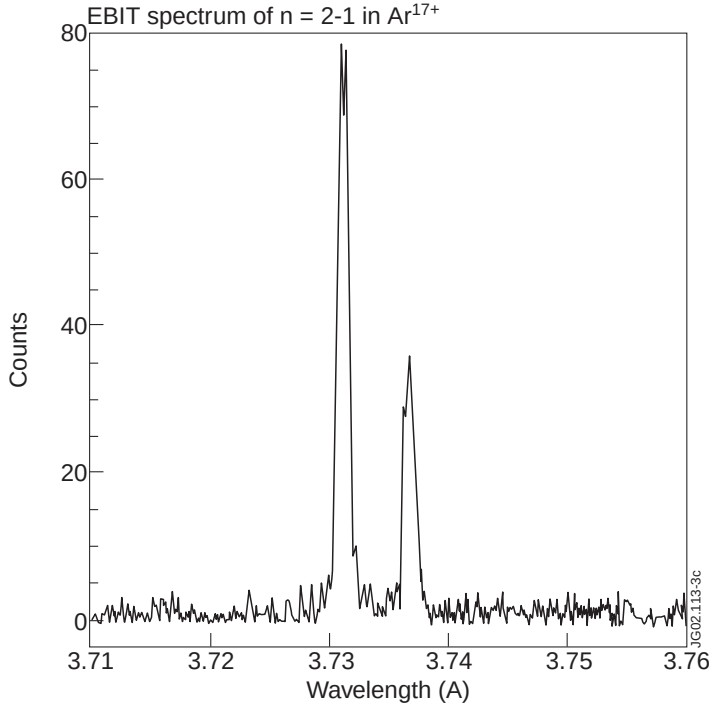

a) **Experimental Ar XVIII Lyα_1 with Gaussian fit.**

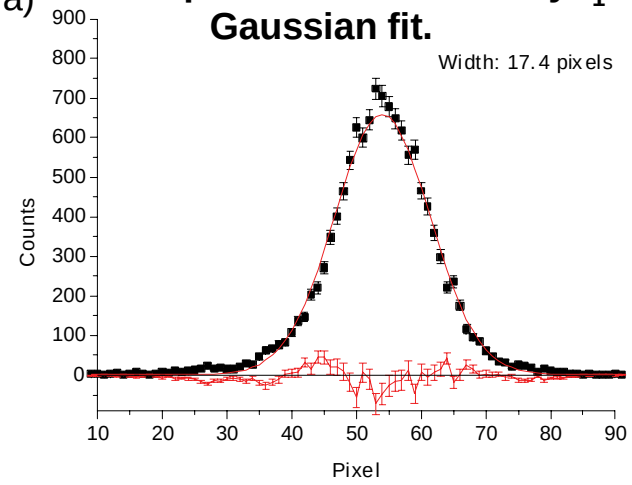

b) **Calculated point spread function of CCD spectrometer.**

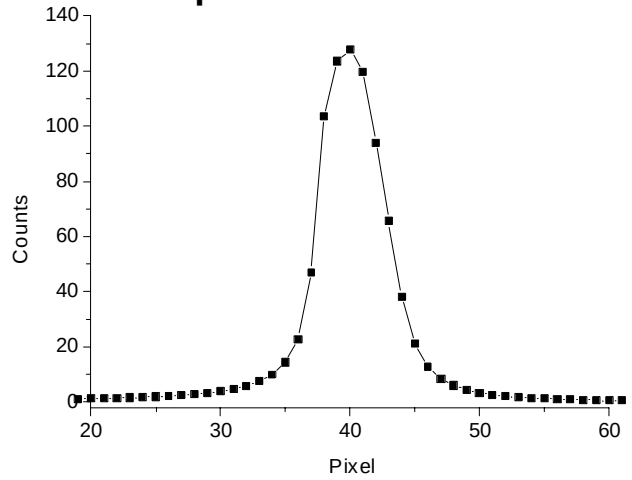

c) **Gaussian de-convolution of a) with b).**

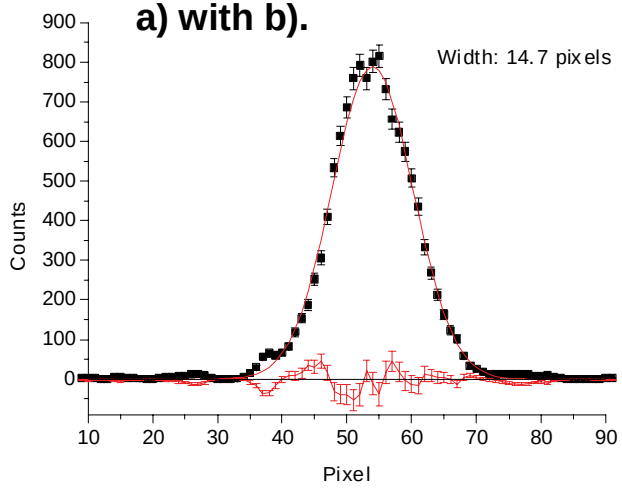

The FWHM of the fitted Gaussian implies a Doppler limited resolution of $\Delta\lambda/\lambda = 3.3 \times 10^{-4}$ and an equivalent ion temperature of 734 eV. The overall instrument resolving power is calculated to be $\lambda/\Delta\lambda_{INST} = 7600$ which is not far short of the theoretical resolving power of the Si(111) crystal itself.

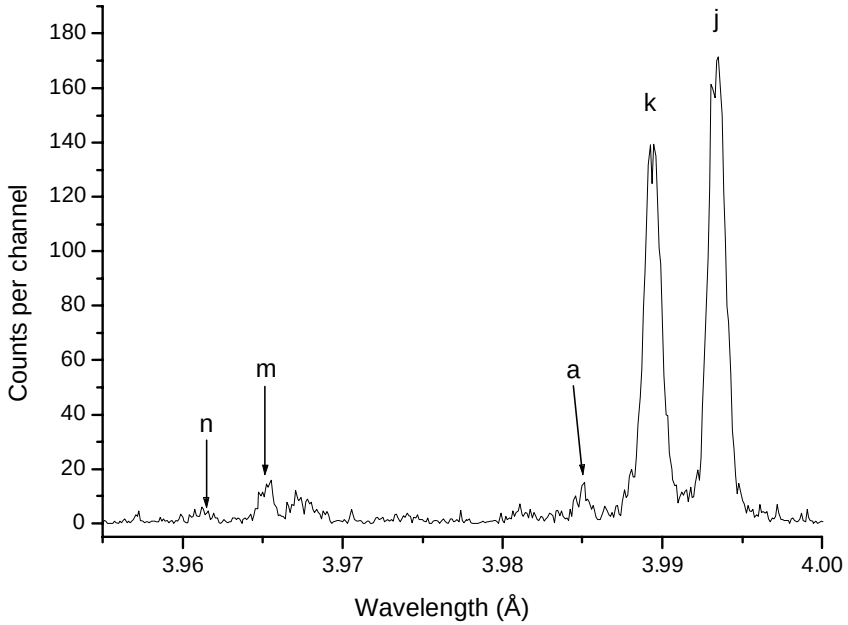

Dielectronic excitation of transitions of type $1s2p^2 – 1s^2p$ at an electron beam energy of 2.24 keV.

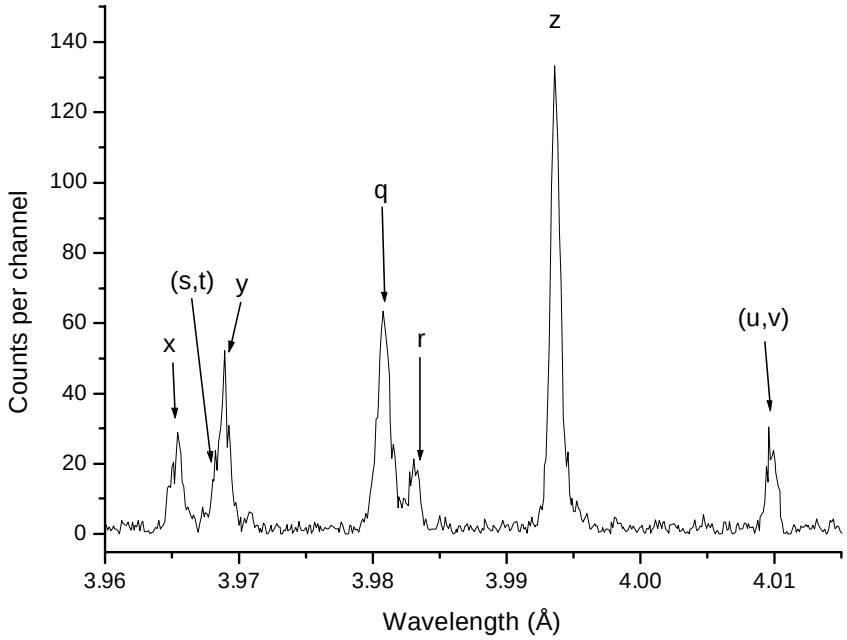

Direct excitation of Ar $^{16+}$ and inner-shell transitions of Ar $^{15+}$ at an electron beam energy of 4.1keV.

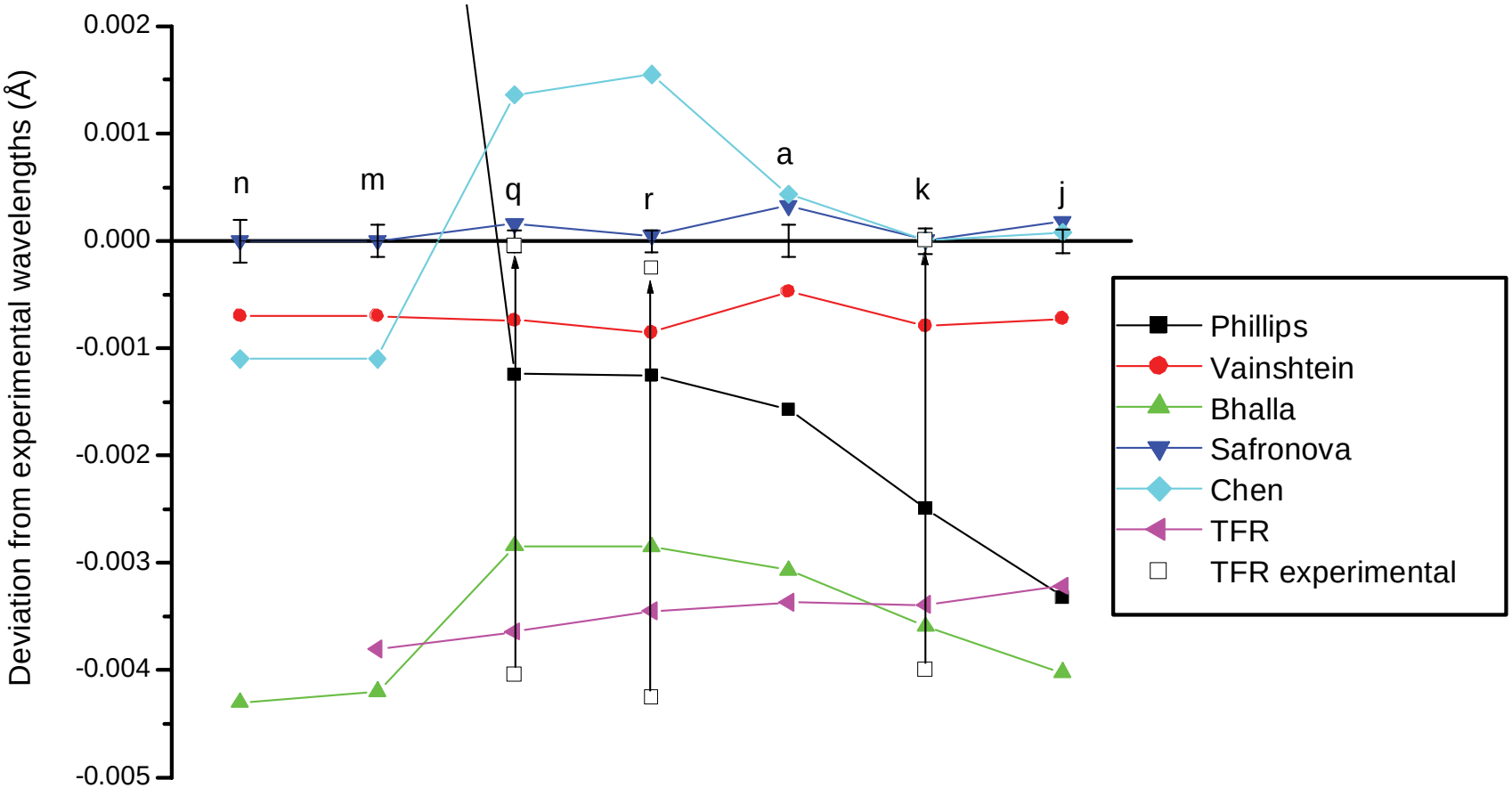

Theory Including radiative and higher order relativistic corrections by Safranova et al. (1995) fit the Oxford EBIT data best.

Role of EBIT

- **"Ground-based" (i.e. neutron damage –free) station which provides standards of emission coefficients and emission line profiles with which to monitor and evaluate ITER spectroscopic diagnostics. Polarisation corrections.**

- **Precision wavelengths and differences $\Delta\lambda$ from nearby wavelength standards such as absorption edges and characteristic diode lines. Small plasma rotational velocities ≥ 1 kms^{-1} derived using $\Delta\lambda$.**

- **Line identifications. At present, low $W^{+6} \rightarrow W^{+20}$ are of great interest.**

- **Charge exchange "distortions" to basic spectra due to collisions with ground and excited state (n=2) neutrals (from beams in ITER).**

- **Forbidden lines in high Z ions.**

* **Collision rate coefficients**